

Cite this: *Dalton Trans.*, 2017, **46**,
12339Facile activation of alkynes with a boraguanidinato-
stabilized germylene: a combined experimental and
theoretical study†Jiří Böserle,^a Grigory Zhigulin,^b Petr Štěpnička,^c Filip Horký,^c Milan Erben,^a
Roman Jambor,^a Aleš Růžička,^a Sergej Ketkov^{*b} and Libor Dostál^{*a}

A boraguanidinato-stabilized germylene, [(i-Pr)₂NB(N-2,6-Me₂C₆H₃)₂Ge], reacts with alkynes RC≡CR selectively in a 2 : 1 molar ratio to afford 3,4-R,R'-1,2-digermacyclobut-3-enes **1a–e** as the products of formal [2 + 2 + 2] cyclization [R/R' = Me/Me (**1a**), Ph/Ph (**1b**), Ph/H (**1c**), t-Bu/H (**1d**) and Cy/H (**1e**)]. Ferrocenyl-substituted alkynes react similarly, yielding the corresponding ferrocenylated 3,4-R,R'-1,2-digermacyclobut-3-enes **2a–d** [where R/R' = Fc/H (**2a**), Fc/Me (**2b**), Fc/Ph (**2c**), and Fc/Fc (**2d**); Fc = ferrocenyl]. By contrast, only one of the triple bonds available in conjugated diynes RC≡CC≡CR is activated with the germylene, while the second one remains intact even in the presence of an excess of the germylene. The exclusive formation of 3,4-R,(C≡CR)-1,2-digermacyclobut-3-enes **3a–c** [R = Ph (**3a**), t-Bu (**3b**), and Fc (**3c**)] was ascribed to a steric repulsion around the second triple bond. On the other hand, the reaction of the germylene with more flexible dialkyne fc(C≡CPh)₂ (fc = ferrocene-1,1'-diyl) proceeded in the expected manner, producing compound **4**, where both triple bonds are transformed into 1,2-digermacyclobut-3-ene rings by reaction with four equivalents of the germylene. All compounds were characterized by multinuclear NMR spectroscopy, Raman and IR spectroscopy, and in the case of **1a–c**, **2a**, **2c**, **3a**, **3b** and **4**, also by single-crystal X-ray diffraction analysis. The ferrocenyl substituted compounds were studied by cyclic voltammetry (CV). Finally, the plausible reaction pathway was studied for a model reaction of [(i-Pr)₂NB(N-2,6-Me₂C₆H₃)₂Ge] with MeC≡CMe using DFT computations.

Received 29th May 2017,
Accepted 23rd August 2017

DOI: 10.1039/c7dt01950e

rsc.li/dalton

Introduction

Germynes, as members of the tetrelene-family, have since Lappert's landmark¹ discoveries developed into an attractive area of main group chemistry.² Thanks to the presence of both the lone pair and π -type empty orbital at the Ge atom, they often exhibit interesting and unexpected reactivity. Some of them were shown to efficiently activate various small molecules.³ The activation of dihydrogen and ammonia by a sterically shielded germylene reported by Power *et al.*^{3i,j} represents

one of the most important initial cornerstones in this area. Similarly, the formal dimers of germynes, digermynes, display remarkable reactivity that is connected with the presence of the Ge=Ge bond.^{2b,4} The reactivity of germynes and digermynes toward unsaturated substrates such as carbonyl compounds or alkynes and investigation of the corresponding reaction mechanisms is an interesting and rapidly developing area.⁵

The treatment of digermynes with alkynes produces 1,2-digermacyclobut-3-enes.^{5,6} Regarding the reactivity of germynes with alkynes, the initial studies were mainly focused on trapping elusive *in situ* generated germynes such as Me₂Ge or on the reactivity of sterically shielded germynes.⁷ These reactions often led to diverse products whose formation was sensitive to both reaction conditions and substrates.⁷ Nevertheless, some of the reactions produced defined and isolable 1,2-digermacyclobut-3-enes.⁸ These cyclic compounds are rarely accessible *via* alternative routes such as the reduction of properly substituted bis(chlorodialkylgermyl)ethenes⁹ or the irradiation of hexa-*tert*-butylcyclotrigermane in the presence of PhC≡CH.¹⁰ Krebs and Veith *et al.*¹¹ showed that a 1,2-digermacyclobut-3-ene or a 1,2-distannacyclobut-3-ene may also be

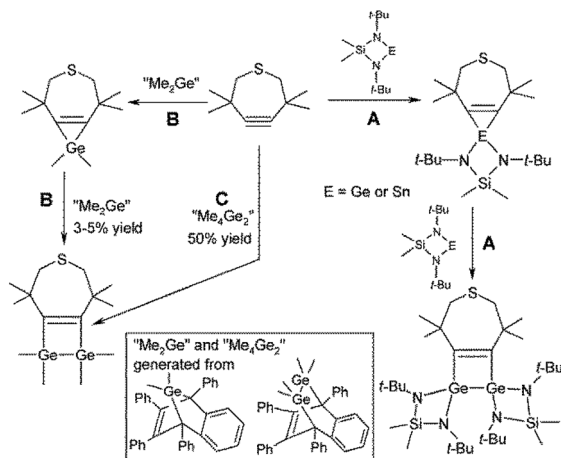
^aDepartment of General and Inorganic Chemistry, Faculty of Chemical Technology, University of Pardubice, Studentská 573, CZ-532 10 Pardubice, Czech Republic.

E-mail: libor.dostal@upce.cz; Fax: +420466037068; Tel: +420466037163

^bG. A. Razuvaev Institute of Organometallic Chemistry RAS, 49 Tropinin St., 603950 Nizhny Novgorod, Russian Federation. E-mail: sketkov@iomc.ras.ru

^cDepartment of Inorganic Chemistry, Faculty of Science, Charles University, Hlavova 2030, CZ-12840 Prague, Czech Republic

†Electronic supplementary information (ESI) available: Table S1 summarizing the crystallographic data, Tables S2 and S3, Schemes S1 and S2, and Fig. S1–S4 showing further computational results. CCDC 1533462–1533469. For ESI and crystallographic data in CIF or other electronic format see DOI: 10.1039/c7dt01950e



Scheme 1 Divergent reactivity of thiacycloheptyne with germylenes and digermenes.

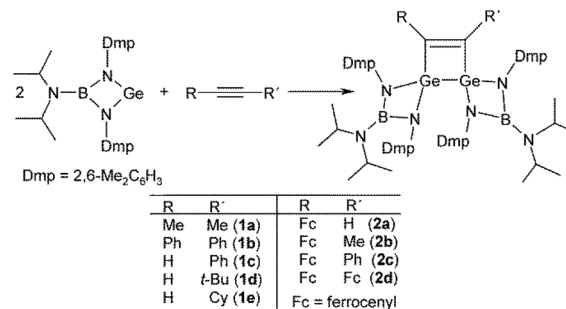
prepared by the reaction of a stable monomeric germylene (or stannylene) supported by a chelating bis-amido ligand $[\text{Me}_2\text{Si}(\text{N}t\text{-Bu})_2\text{E}]^{12}$ ($\text{E} = \text{Ge}$ or Sn) and a thiacycloheptyne (Scheme 1A). In this case, the authors suggested an initial formation of the corresponding three-membered rings (*i.e.* stannirene or germirene) and its subsequent reactions with the second molecule of the tetraylene leading to 1,2-digermacyclobut-3-ene or 1,2-distannacyclobut-3-ene. Interestingly, the same reaction using *in situ* generated germylene Me_2Ge led to the formation of a stable germirene,¹³ whose structure was later established by X-ray diffraction analysis.¹⁴ Treatment of this germirene with *in situ* generated Me_2Ge provided 1,2-digermacyclobut-3-ene in negligible yield (Scheme 1B).^{7a} By contrast, thiacycloheptyne was smoothly converted to 1,2-digermacyclobut-3-ene upon reacting with Me_4Ge_2 and the cyclic product could be isolated in 50% yield by sublimation (Scheme 1C).^{7a} This finding proves the importance of the germanium precursor and also indicates that the germanium(II) centre incorporated within a strained four-membered ring (Scheme 1A) may provide access to 1,2-digermacyclobut-3-ene rings.

However, to the best of our knowledge, no comprehensive study dealing with a tailored preparation of 1,2-digermacyclobut-3-enes starting from a similar *N,N*-chelated germylene has been performed so far. In this work, we report the reactivity of the boraguanidinato-stabilized germylene, $[(i\text{-Pr})_2\text{NB}(N\text{-}2,6\text{-Me}_2\text{C}_6\text{H}_3)_2]\text{Ge}$,¹⁵ toward various alkynes and diynes affording a whole set of substituted 1,2-digermacyclobut-3-enes including those substituted with the redox active ferrocenyl moieties. The plausible mechanism of this particular cyclization reaction was studied from the theoretical viewpoint by DFT computations.

Results and discussion

Syntheses, characterization and structure of studied compounds

Addition of the germylene, $[(i\text{-Pr})_2\text{NB}(N\text{-}2,6\text{-Me}_2\text{C}_6\text{H}_3)_2]\text{Ge}$, to simple alkynes $\text{RC}\equiv\text{CR}'$ (Scheme 2) resulted in a formal $[2 + 2 + 2]$



Scheme 2 Synthesis of 1a–e and 2a–d.

cyclization involving the alkyne and 2 equiv. of the germylene to afford the respective 3,4- $\text{R,R}'$ -1,2-digermacyclobut-3-enes **1a–e**, where $\text{R/R}' = \text{Me/Me}$ (**1a**), Ph/Ph (**1b**), Ph/H (**1c**), $t\text{-Bu/H}$ (**1d**), and Cy/H (**1e**). Analogously, the ferrocene substituted 3,4- $\text{R,R}'$ -1,2-digermacyclobut-3-enes **2a–d** [$\text{R/R}' = \text{Fc/H}$ (**2a**), Fc/Me (**2b**), Fc/Ph (**2c**), and Fc/Fc (**2d**); $\text{Fc} = \text{ferrocenyl}$] were smoothly obtained by the reaction of corresponding alkynes $\text{FcC}\equiv\text{CR}'$ with 2 equiv. of the parent germylene (Scheme 2).

All products were isolated as crystalline solids by crystallization from hexane in moderate to good yields (31–77%), the lower yields in some cases being caused by their high solubility even at low temperatures (note: the compounds are also well soluble in aromatic solvents). Notably, all attempts to react the alkynes with only 1 equiv. of the germylene and trap a plausible germirene intermediate failed (see the discussion of the reaction mechanism below). The compounds were

Table 1 Selected ^1H and $^{13}\text{C}\{^1\text{H}\}$ NMR chemical shifts [ppm] of studied compounds acquired in C_6D_6 at 25 °C

Compound	i-Pr-CH		Dmp-CH ₃		C=C	C≡C
	$\delta(^1\text{H})$	$\delta(^{13}\text{C})$	$\delta(^1\text{H})$	$\delta(^{13}\text{C})$	$\delta(^{13}\text{C})$	$\delta(^{13}\text{C})$
1a	3.14	46.2	2.28, 2.47	19.9, 20.5	172.2	—
1b	3.14	46.2	2.23, 2.42	20.5, 20.7	176.3	—
1c	3.16	46.2	2.16, 2.37	19.9, 20.2	160.2	—
1d	3.18	46.1	2.42, 2.44	20.7, 20.8	182.8	—
		46.5	2.30, 2.38	20.2, 20.5	156.0	
1e	3.15	46.1	2.51, 2.53	20.6, 21.1	198.0	—
			2.30, 2.36	19.9, 20.0	157.6	
2a	3.17	46.2	2.47, 2.49	20.3, 20.5	192.8	—
			2.33, 2.35	19.8, 20.4	155.8	
2b	3.20	46.3	2.49, 2.53	20.4, 21.2	181.0	—
		46.3	2.33, 2.39	20.3, 20.8 ^a	168.3	
2c	3.12	46.3	2.54 ^a	21.6	170.9	—
		46.3	2.27, 2.35	20.8, 21.1	169.8	
2d	3.28	46.5	2.41, 2.73	21.8, 23.4	171.8	—
		46.3	2.40 ^a	21.3, 21.8	163.7	
3a	3.18	46.2	2.15, 2.39	20.2, 20.6	153.1	88.4
3b	3.21	46.3	2.46, 2.72	20.8, 20.9	180.4	108.7
		46.6	2.55, 2.74	21.4, 21.7	193.6	120.4
3c	3.22	46.3	2.35, 2.38	20.1, 20.6	148.1	87.2
		46.4	2.59, 2.81	21.2, 21.5	177.2	110.4
4	3.09	46.2	2.22, 2.31	20.9, 21.0	169.9	—
		3.25	2.36, 2.59	21.1, 21.6	170.6	

^a Two overlapping signals.



Table 2 The solid-state Raman and IR data (in cm^{-1}) for studied compounds

Compound	$\nu_{\text{C}=\text{C}}$		$\nu_{\text{C}\equiv\text{C}}$		$\nu_{\text{C}\cdots\text{C}}^a$	
	Ra	IR	Ra	IR	Ra	IR
1a	1547m	n.o.	—	—	—	—
1b	1557m	n.o.	—	—	—	—
1c	1514s	n.o.	—	—	—	—
1d	1517m	n.o.	—	—	—	—
1e	1511m	n.o.	—	—	—	—
2a	1521 vs	1519m	—	—	1111s	1109m
2b	1549s	1547w	—	—	1108s	1108m
	1537s ^b	1537w ^b				
2c	1535vs	1535m	—	—	1108s	1107m
2d	1539vvs	1537w	—	—	1108s	1107s
3a	1539m	n.o.	2191vs	2191w	—	—
3b	1512m	n.o.	2264m	2179w	—	—
			2180vs ^b			
3c	1528vs	1528w	2217m	2175m	1107s	1107s
			2175vs ^b			
4	1537vs	1537w	—	—	—	—

^a The “ring-breathing” mode of the $\text{Fe}(\eta^5\text{-C}_5\text{H}_5)$ fragment. ^b The band is split due to site-symmetry effects in the solid state.

characterized by ^1H and $^{13}\text{C}\{^1\text{H}\}$ NMR spectroscopy (Table 1). In each case, the spectra revealed one set of signals due to the substituents R and R'.

Furthermore, signals typical for the $\text{C}=\text{C}$ carbons of the central 1,2-digermacyclobut-3-ene ring were detected in $^{13}\text{C}\{^1\text{H}\}$ NMR spectra (*i.e.* one signal for symmetric structures **1a**, **1b**, and **2d** at $\delta(^{13}\text{C}) = 163.7\text{--}176.3$ ppm and two signals for their nonsymmetric counterparts **1c–e** and **2a–c** at $\delta(^{13}\text{C}) = 155.1\text{--}198.0$ ppm). Importantly, these signals are shifted significantly to lower fields compared to the starting alkynes to positions similar to those of the related 1,2-digermacyclobut-3-enes.^{7f,9,10} In addition, an expected set of signals was detected for the boraguanidinato ligand including the resonances of the (i-Pr)₂N and 2,6-Me₂C₆H₃ (Dmp) moieties. Two singlets for the Me groups (^1H and ^{13}C NMR spectra) and six signals for the aromatic carbons of the Dmp groups were detected for the symmetric structures (**1a**, **1b**, **2d**), because the methyl groups of Dmp are magnetically non-equivalent, one being orientated toward the 1,2-digermacyclobut-3-ene ring, while the second one points outside this ring (*i.e.* the structure in the solid state is most probably retained in solution *vide infra*). Consequently, four singlets for the methyl groups of Dmp and twelve signals for aromatic carbons were observed for the non-symmetric compounds (**1c–e**, **2a–c**; Table 1), because the symmetry of the central 1,2-digermacyclobut-3-ene is lost due to the presence of two different R and R' substituents. Furthermore, the NMR spectra of **2a–2d** displayed the characteristic signals of the ferrocenyl moieties (see the Experimental section). The presence of the $\text{C}=\text{C}$ bond in the four-membered digermacycle was further evidenced by Raman spectroscopy. It is well known that cyclobutene and its derivatives show characteristic $\text{C}=\text{C}$ stretching bands (weak in infrared but medium-to-strong intensity in Raman spectra) in the region $1520\text{--}1600\text{ cm}^{-1}$.¹⁶ However, relevant data for heterocyclic systems structurally related to our digermacyclobutenes are relatively sparse, the

Raman spectra being reported only for several derivatives of 1,2-diosmacyclobut-3-ene ($\approx 1500\text{ cm}^{-1}$), 1,2-palladastannacyclobut-3-ene ($\approx 1466\text{ cm}^{-1}$), 1,2-disilacyclobut-3-ene ($1558\text{--}1610\text{ cm}^{-1}$) and 3,4-bis(trifluoromethyl)-1,2-diselenete (1616 cm^{-1}).¹⁷ In the Raman spectra of complexes **1–4** (Table 2), the band attributable to the $\text{C}=\text{C}$ stretching vibration was clearly detected in the range $1511\text{--}1549\text{ cm}^{-1}$. The variation in the frequency of this band could be attributed to both the electronic influence of the double bond substituents and to the geometric strain of 1,2-digermacyclobut-3-ene in the particular compound. Besides, complexes **2a–2d** showed an intense Raman line at $1110 \pm 2\text{ cm}^{-1}$ attributable to the “ring-breathing” mode of the unsubstituted η^5 -coordinated cyclopentadienyl ring.¹⁸

The formulation of **1a–c** (Fig. 1), **2a** and **2c** (Fig. 2) was unambiguously corroborated by single crystal X-ray diffraction analysis. The determined molecular structures are quite

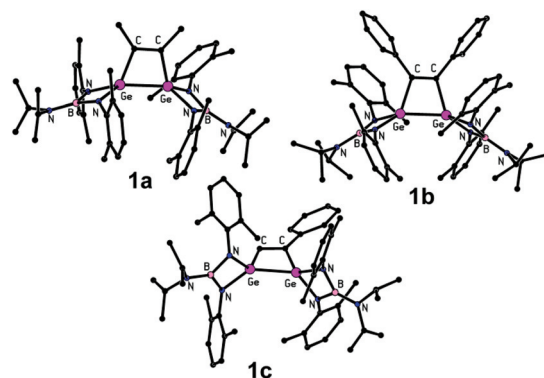


Fig. 1 Molecular structures of **1a–c**. Hydrogen atoms are omitted for clarity. Only one of the four independent molecules of **1c** is presented and, in the case of **1a** and **1c**, only one position for the disordered i-Pr and Dmp groups is shown.



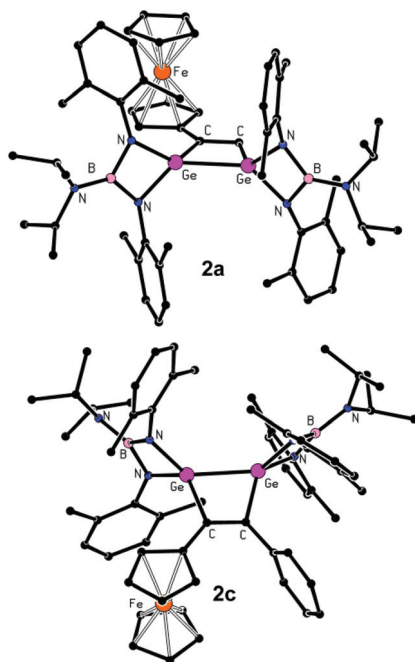


Fig. 2 Molecular structures of **2a** and **2c**. Hydrogen atoms and the hexane solvate molecule in the case of **2c** are omitted for clarity.

similar and, hence, will be described jointly. The central four-membered digermacyclobut-3-ene ring is nearly planar and the C=C distances (1.337(4)–1.356(9) Å, see Table 3) clearly prove the presence of a double bond, especially when compared with $\Sigma_{\text{rcov}}(\text{C}=\text{C}) = 1.34$ Å.¹⁹ The Ge–C separations within these rings span the range 1.945(3)–1.995(4) Å, suggesting the presence of covalent Ge–C bonds (cf. $\Sigma_{\text{rcov}}(\text{Ge},\text{C}) = 1.96$ Å).

By contrast, the Ge–Ge bonds (2.4426(6)–2.5029(5) Å) appear elongated in comparison with $\Sigma_{\text{rcov}}(\text{Ge},\text{Ge}) = 2.42$ Å, but are fully comparable with the Ge–Ge distances in structurally

related analogues such as 1,1,2,2-(i-Pr)₄-3-Ph-1,2-digermacyclobut-3-ene (2.439(7) Å),⁹ 1,1,2,2-(*t*-Bu)₄-3-Ph-1,2-digermacyclobut-3-ene (2.531(6) Å),^{10a} 1,2-dihydro-1,2-[(Me₃Si)₃C]₂-3,4-Ph₂-1,2-digermacyclobut-3-ene (2.514(2) Å)^{7f} and, particularly, the closest analogue, which is Veith's 1,2-digermacyclobut-3-ene (Scheme 1A; 2.549(1) Å).¹¹ Bond angles within the C₂Ge₂ rings are significantly more acute at the germanium atoms (72.60(10)–74.07(17)°) than at the carbon atoms (105.1(2)–109.3(2)°) reflecting the distortion of the four-membered ring by the longer Ge–Ge bonds. The coordination environment of the germanium atoms in **1a–c**, **2a** and **2c** may be described as strongly distorted tetrahedral and the central Ge atoms are effectively chelated and shielded by the boraguanidinato ligand. The Ge–N bond lengths in the range 1.846(2)–1.866(3) Å are within the expected range (cf. $\Sigma_{\text{rcov}}(\text{Ge},\text{N}) = 1.92$ Å).¹⁹

In contrast to simple internal alkynes, only one of the triple bonds available in conjugated diynes RC≡CC≡CR is attacked by the germylene as exemplified by the preparation of 3,4-R, (C≡CR)-1,2-digermacyclobut-3-enes **3a–c**, where R = Ph (**3a**), *t*-Bu (**3b**), and Fc (**3c**) (Scheme 3A). It is noteworthy, that even heating of isolated **3a–c** with an excess of the germylene did not lead to the formation of the second four-membered digermacyclobutadiene ring, which can be explained by a significant steric hindrance at the unreacted C≡C bond (see the following discussion, Fig. 3).

The ¹H and ¹³C{¹H} NMR spectra of **3a–c** (Table 1) were similar to those described above for **1a–e** and **2a–d** and in line with the proposed structures. The presence of an intact C≡C bond was manifested through a pair of triple bond signals in the ¹³C{¹H} NMR spectra ($\delta(^{13}\text{C}) = 78.2$ –120.4 ppm), whereas the C=C moiety within the 1,2-digermacyclobut-3-ene rings gave rise to two signals at $\delta(^{13}\text{C}) = 153.1$ –193.6 ppm. The presence of the C=C and C≡C bonds in **3a–3c** was further evidenced by strong Raman lines at 1512–1539 cm^{−1} and 2175–2191 cm^{−1}, respectively. The Raman and IR spectrum of **3c** also showed a strong band at 1107 cm^{−1} due to the ring-

Table 3 Selected bond lengths [Å] and bonding angles [°] in studied compounds

Compound	Bond lengths [Å]					Bonding angles [°]	
	Ge–Ge	Ge–N	Ge–C	C=C	C'≡C'	C–Ge–Ge	C=C–Ge
1a	2.4426(7)	1.854(3), 1.856(3) 1.858(2), 1.859(3)	1.975(3) 1.974(3)	1.341(4)	—	73.61(9), 73.85(9)	106.3(2), 105.9(2)
1b	2.4427(8)	1.860(3), 1.860(3) 1.845(2), 1.855(3)	1.988(4) 1.985(4)	1.337(4)	—	73.46(10), 73.72(9)	106.1(3), 105.3(3)
1c	2.4572 ^a	1.852 ^a	1.972 ^a	1.337 ^a	—	73.43 ^a	106.4 ^a
2a	2.5029(5)	1.864(2), 1.857(2) 1.866(3), 1.864(2)	1.987(3) 1.945(3)	1.341(5)	—	72.98(10), 72.60(10)	109.3(2), 105.1(2)
2c	2.4471(8)	1.860(4), 1.864(4) 1.865(4), 1.856(5)	1.991(6) 1.995(4)	1.347(7)	—	73.63(15), 74.09(13)	106.4(3), 105.2(3)
3a	2.4682(7)	1.855(3), 1.846(3) 1.859(3), 1.848(3)	1.995(3) 1.975(3)	1.349(4)	1.186(5)	72.46(10), 74.50(8)	107.2(2), 105.0(2)
3b	2.4227(7)	1.861(2), 1.863(2) 1.863(2), 1.854(2)	1.986(3) 1.997(3)	1.347(4)	1.192(5)	73.55(9), 74.38(9)	104.7(2), 105.3(2)
4	2.4504(9)	1.869(5), 1.868(6) 1.861(5), 1.865(5)	1.985(6) 1.973(6)	1.346(8)	—	73.44(19), 73.95(15)	106.0(4), 106.0(4)

^a Average value for four independent molecules in the unit cell is given.



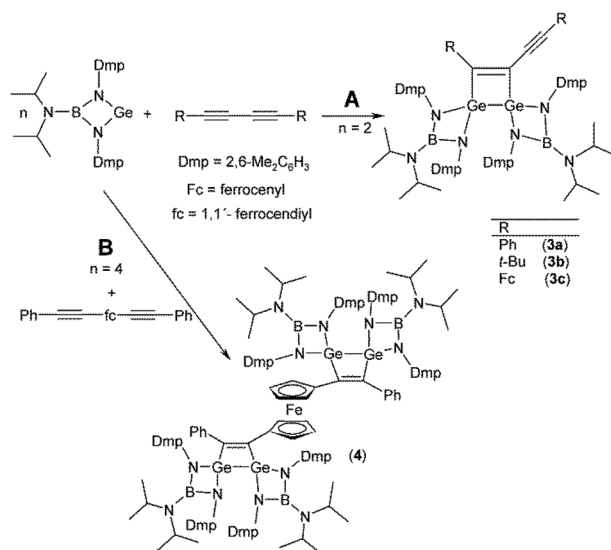
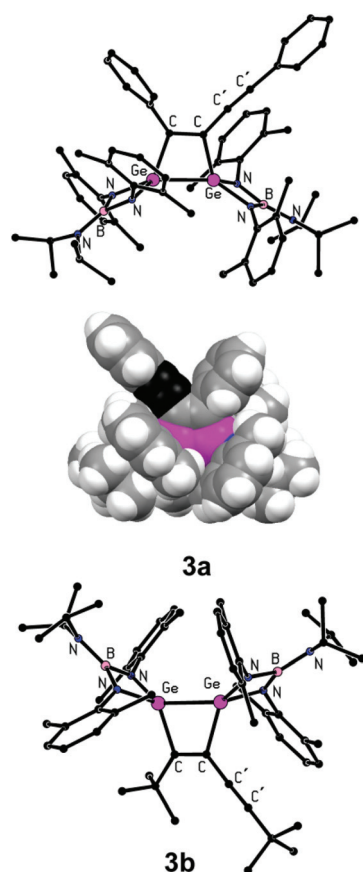
Scheme 3 Synthesis of **3a–c** and **4**.

Fig. 3 Molecular structure of **3a** (including a space-filling model manifesting the steric protection of the intact C≡C bond – in black) and **3b**. Hydrogen atoms and the hexane solvate molecule in the case of **3a** are omitted for clarity. Only one position for the disordered *i*-Pr group in **3a** and *t*-Bu group in **3b** is shown.

breathing mode of the $\text{Fe}(\eta^5\text{-C}_5\text{H}_5)$ fragment. The molecular structures of **3a** and **3b** determined by single-crystal X-ray diffraction analysis (Fig. 3) confirm the presence of intact C≡C bonds in the structures (C–C bond lengths: 1.187(5) and 1.182(7) Å in **3a** and **3b**, respectively; *cf.* $\Sigma_{\text{rcov}}(\text{C}\equiv\text{C}) = 1.2$ Å (ref. 19)) and the formation of one 1,2-digermacyclobut-3-ene ring. The C=C bond lengths within the cycle of 1.349(4) and 1.347(7) Å for **3a** and **3b**, respectively, are comparable to those in **1a–c**, **2a** and **2c** and their analogues.^{7f,9–11} Similarly, the Ge–Ge bond lengths 2.4682(6) (**3a**) and 2.4207(8) (**3b**) Å approach the values found in **1a–c**, **2a** and **2c** and even the coordination spheres around the germanium atoms are very similar (see Table 3).

In order to elicit the simultaneous addition of germylene, $[(i\text{-Pr})_2\text{NB}(N\text{-}2,6\text{-Me}_2\text{C}_6\text{H}_3)_2]\text{Ge}$, across two C≡C bonds in one molecule, we turned our attention to a diyne with a flexible backbone, 1,1'-bis(phenylethynyl)ferrocene, $\text{fc}(\text{C}\equiv\text{CPh})_2$ (fc = ferrocene-1,1'-diyl). Indeed, when treated with four molar equivalents of the germylene (Scheme 3B), this diyne smoothly reacted at both its C≡C bonds and was converted to complex **4** comprising two chemically equivalent 1,2-digermacyclobut-3-ene rings. The $^{13}\text{C}\{^1\text{H}\}$ NMR spectra of **4** displayed two signals at $\delta(^{13}\text{C}) = 169.9$ and 170.6 ppm due to the C=C bond but no signals attributable to a C≡C bond. The presence of the bridging ferrocene unit was reflected through a pair of signals of the Cp protons ($\delta(^1\text{H}) = 3.37$ and 4.30 ppm) in the ^1H NMR spectrum and three resonances in the $^{13}\text{C}\{^1\text{H}\}$ NMR spectrum ($\delta(^{13}\text{C}) = 73.5$, 74.7 ($2 \times \text{CH}$), and 79.2 (C_{ipso}) ppm). In addition, two sets of signals were observed for two magnetically non-equivalent boraguanidate ligands (Table 1 and Experimental section). A very strong Raman line at 1537 cm^{-1} and a weak IR band at the same position attested to the presence of the C=C bond in the 1,2-digermacyclobut-3-ene ring.

Compound **4** crystallizes in the centrosymmetric space group $P\bar{1}$ and with the central iron atom residing on an inversion centre. Its molecular structure is presented in Fig. 4. The two structurally equivalent 1,2-digermacyclobut-3-ene rings in the structure of **4** are nearly ideally planar. The heterocycles facing in mutually opposite directions, minimizing their possible steric interactions. The C=C (1.350(14) Å) and Ge–Ge (2.4504(15) Å) distances in **4** compare well with the respective parameters discussed above (Table 3). Likewise, the Ge–N distances fall into an expected interval 1.861(8)–1.873(8) Å.

Electrochemical measurements

The electrochemical behaviour of ferrocenyl-containing derivatives **2a–d**, **3c** and **4** was studied by cyclic voltammetry (CV; in dichloromethane containing 0.1 M $\text{Bu}_4\text{N}[\text{PF}_6]$). Redox potentials are given in Table 4 and the representative voltammograms are shown in Fig. 5 and 6. The cyclic voltammetric response of compounds **2a–d** is generally similar (Fig. 5). The compounds undergo a reversible oxidation, which is followed by an irreversible multielectron redox event at more positive potentials. This first redox process, attributed to the oxidation of the ferrocene substituent, is controlled by diffusion ($i_{\text{pa}} \propto \nu^{1/2}$; i_{pa} and ν stand for anodic peak potential and scan rate, respectively) and corresponds to a one-electron exchange. For



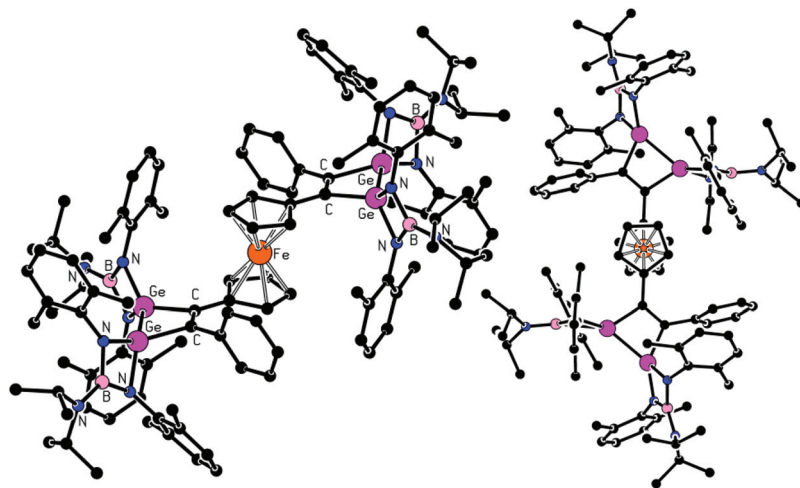


Fig. 4 Molecular structure of **4**. Hydrogen atoms and the toluene solvate molecule are omitted for clarity.

Table 4 Electrochemical data for **2a–d**, **3c** and **4**^a

Compound	First oxidation $E^{\circ'}$ [V]	Second oxidation E_{pa} [V]
2a	0.11	0.77
2b	0.09	0.87
2c	0.10	0.86
2d	0.03, 0.28	0.98
3c	0.08, 0.24	0.88
4	0.20	0.88

^a Data in dichloromethane/0.1 M Bu₄N[PF₆] at room temperature. Scan rate: 100 mV s⁻¹. Potentials were recorded against internal decamethylferrocene/decamethylferrocenium and converted to the ferrocene/ferrocenium scale (see the Experimental section). $E^{\circ'}$ denotes formal potential determined as an average of anodic (E_{pa}) and cathodic (E_{pc}) peak potentials in cyclic voltammetry.

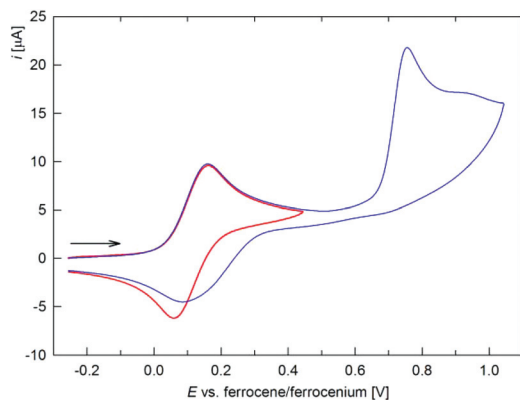


Fig. 5 Full (blue) and partial (red) cyclic voltammogram of **2a**. The arrow indicates the scan direction (scan rate: 100 mV s⁻¹, glassy carbon electrode, CH₂Cl₂).

all compounds, the redox potentials of the first oxidation are more positive than that of ferrocene itself, suggesting an overall electron-withdrawing nature of the digermacyclobuta-

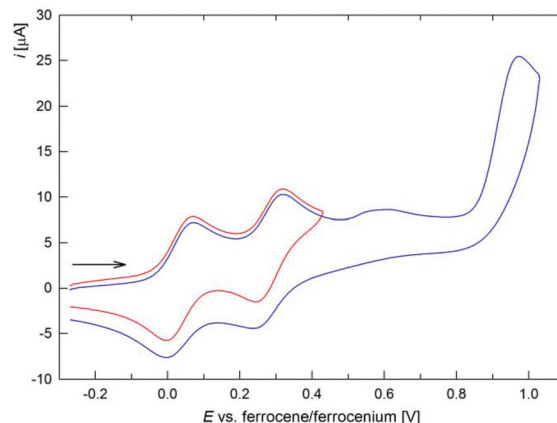


Fig. 6 Full (blue) and partial (red) cyclic voltammograms of **2d**. The arrow indicates the scan direction (scan rate: 100 mV s⁻¹, glassy carbon electrode, CH₂Cl₂).

diene ring, and are only slightly affected by the other substituent R in the C(Fc)=C(R) moiety (R = H, Me, Ph). Compound **2d** bearing two ferrocene substituents at the C=C double bond is oxidized in two separated reversible steps (Fig. 6) and a multielectron process at higher potentials (Table 4). The sequential oxidation of the chemically equivalent ferrocene moieties indicates their electronic communication between the ferrocene units. The calculated comproportionation constant²⁰ $K_{com} \sim 18\,000$ allows ranking the electrochemically generated monocation **2d**⁺ as partly delocalized (class II) in the Robin–Day classification.²¹ Notably, the separation of the redox waves in **2d** is substantially higher (0.25 V) than in FcC≡Cfc and *cis*-FcC≡Cfc (ca. 0.12 V),²² indicating a stronger electronic communication in the digermacyclobutadiene derivative. Two successive initial oxidations are observed also in the CV of **3c**. In this case, however, the oxidations are due to the chemically different ferrocenyl groups. Upon comparing the data for the monoferrocenyl derivatives **2a–d**, the first oxi-



dition of **3c** occurring at $E^\circ = 0.11$ V vs. ferrocene/ferrocenium can be tentatively attributed to the ferrocenyl substituent at the four membered ring and the following one at $E^\circ = 0.24$ V to the $\text{FcC}\equiv\text{C}$ moiety. Finally, the CV response of compound **4** in which the ferrocene-1,1'-diyl group interconnects two digermacyclobutadiene rings is similar to that of the simple representatives **2a–c** except that the first reversible oxidation appears shifted to more positive potentials owing to the presence of two electron-withdrawing substituents at the ferrocene unit.

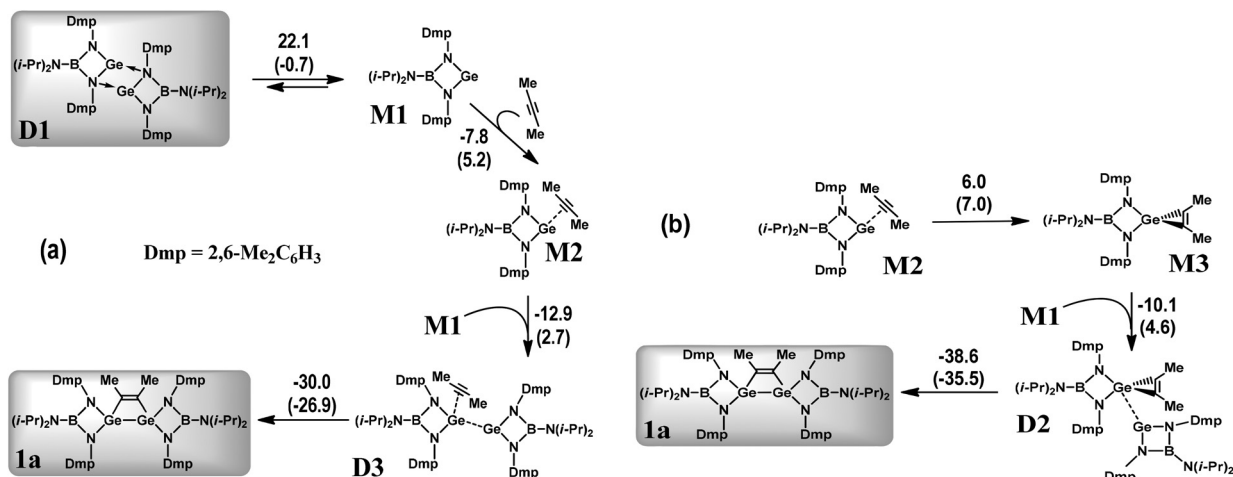
Theoretical considerations

To gain an insight into the plausible reaction mechanism and electronic structures of the species involved a theoretical study has been undertaken. The earlier mechanistic investigations of interactions between alkynes and derivatives of low-valent germanium are mainly represented by DFT calculations of reactions with (di)germenes,^{5a,23} digermynes²⁴ and ylide-like germylene^{2a,25} which result in various types of cycloadditions and acetylene C–H bond activation. The formation of germacyclobutenes was observed with germenes. The diradical, zwitterionic, and concerted pathways were investigated.²³ The addition of alkynes to digermynes led to 1,2-digermacyclobutadienes.²⁴ Notice, however, that the germanium bonding in germenes and digermynes is quite different from the bonding situation in the complexes studied in the present work (*vide infra*). On the other hand, the interaction of zwitterionic N-heterocyclic germylene with HCCR resulted in (4 + 2) cycloadducts and the formation of alkynyl germylene,²⁵ which was not observed in our study.

The elementary reactions accompanying the interaction of germylene, $[(i\text{-Pr})_2\text{NB}(N\text{-}2,6\text{-Me}_2\text{C}_6\text{H}_3)_2]\text{Ge}$ (**M1**), and dimethylacetylene were simulated by DFT calculations at the M06-2X/DGDZVP level of theory in the gas phase as well as in C_6H_6 solution (Scheme 4 and Schemes S1, S2; see the ESI†). Selected

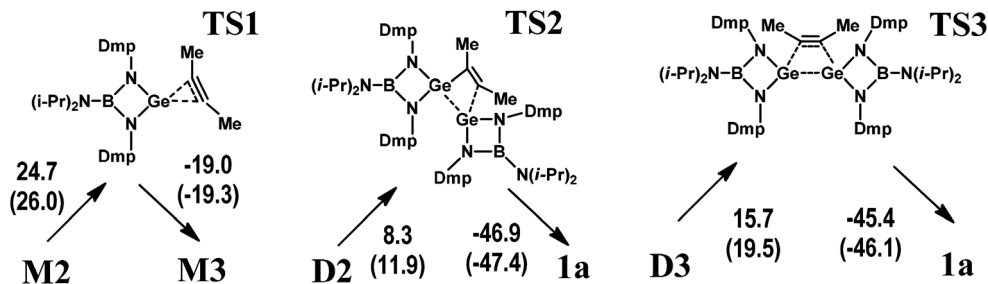
interatomic distances in the optimized gas-phase structures of the corresponding reactants, 3,4- Me_2 -1,2-digermacyclobut-3-ene **1a** and intermediates are given in Table S2.† Generally, the optimized geometries agree very well with the experimental data determined from X-ray structures of **1a** (Table 2) and dimer **D1**.¹⁵ The earlier NMR investigations¹⁵ detected only the monomer **M1** species in solution. On the other hand, in crystal germylene forms dimeric molecules **D1**.¹⁵ An equilibrium involving the **M1** and **D1** species can, therefore, take place in C_6H_6 solution, the concentration of **D1** being much lower than that of **M1** (Scheme 4a). Hence, we analysed interactions of both **M1** and **D1** with C_2Me_2 . Since our computations indicate that the **M1** triplet state is 56.6 kcal mol^{−1} above the closed-shell singlet, the possible reaction mechanisms were simulated on the singlet potential energy surface. To study the electronic structures of selected species the molecular orbital (MO) and natural bond orbital (NBO) analyses as well calculations within Bader's quantum theory of atoms in molecules (QTAIM) were carried out (for details, see the Experimental section).

The initial stage of the reaction between **M1** and C_2Me_2 consists of a coordination of the alkyne to the germylene. In the resulting complex **M2** (Scheme 4a), the linear alkyne donates electron density to the vacant orbital formed by the Ge 3p atomic wavefunction as indicated by NBO analysis (Fig. S1†). For the **M2** species, at least two further reaction pathways are possible: one *via* germirene **M3** (Scheme 4b) with a subsequent addition of a second **M1** molecule (**M2** → **M3** → **D2** → **1a**) and the other *via* the dimer **D3** bearing a weakly bound C_2Me_2 fragment (Scheme 4a). Notably, the former mechanism resembles that described in Scheme 1A.¹² The **M2** → **M3** stage produces germirene **M3** in which the three-membered GeC_2 ring is orthogonal to the GeN_2B cycle and the $\text{C}=\text{C}-\text{CH}_3$ angles are *ca.* 134°. However, this stage is endergonic ($\Delta G = 7.0$ kcal mol^{−1}). The formation of two Ge–C covalent



Scheme 4 DFT-based mechanisms of the 3,4- Me_2 -1,2-digermacyclobut-3-ene **1a** formation *via* the weakly bound C_2Me_2 adducts **M2** and **D3** (a) and *via* germirenes **M3** and **D2** (b). The calculated changes of the electronic and Gibbs (in parentheses) free energies in C_6H_6 solution are given in kcal mol^{−1}.





Scheme 5 Transition states corresponding to the key stages of the **1a** formation mechanisms predicted by DFT. Calculated gas-phase activation energies ΔE_a and Gibbs free energies of activation ΔG^\ddagger (in parentheses) are given in kcal mol⁻¹.

bonds and transformation of alkyne to alkene on going from **M2** to **M3** appears to be accompanied by an increase in the electronic energy ($\Delta E_{el} = 6.0$ kcal mol⁻¹). Moreover, the corresponding gas-phase activation energy (Scheme 5) is rather high ($\Delta E_a = 24.7$ kcal mol⁻¹) which kinetically prevents the formation of germirene **M3**. Therefore, the formation of **1a** via **M3** seems to be hardly probable though the final stage (**D2** → **1a**) is highly exergonic ($\Delta G = -35.8$ kcal mol⁻¹) and the corresponding activation energy is only 8.3 kcal mol⁻¹ (Scheme 5). This explains the failure of our attempts to trap germirene **M3** experimentally (see above).

On the other hand, the interaction of **M2** with the germylene species (**M2** → **D3**) is associated with a decrease in the electronic energy ($\Delta E_{el} = -12.9$ kcal mol⁻¹) and is characterized by a low positive ΔG value (2.7 kcal mol⁻¹). In contrast to the **M2** → **M3** stage, the **D3** dimer transformation into the **1a** product is highly exergonic ($\Delta G = -26.9$ kcal mol⁻¹) and leads to a decrease in the electronic energy ($\Delta E_{el} = -30.0$ kcal mol⁻¹). The **D3** → **1a** gas-phase activation energy (15.7 kcal mol⁻¹, Scheme 5) is much lower than that of the **M2** → **M3** stage. This pathway is, therefore, preferable both thermodynamically and kinetically as compared to that involving intermediate **M3**. Notably, the gas-phase reaction parameters (Scheme S2†) reveal similar trends, being indicative of the same mechanism.

In the course of a DFT search for additional possible reaction pathways other stable digermanium intermediates were found (Schemes S1, S2, Tables S2, S3, Fig. S4; see the ESI†). However, the mechanisms involving these species appeared to be less energetically favourable as compared to the pathway via **M2** and **D3** considered above (Scheme 4a). A detailed analysis of these possible mechanisms is given in the ESI.†

The **D3** intermediate playing a key role in the formation of **1a** (Scheme 4a) can be considered as an adduct of C₂Me₂ and digermene [(i-Pr)₂NB(N-2,6-Me₂C₆H₃)₂GeGe[(i-Pr)₂NB(N-2,6-Me₂C₆H₃)₂]] **D5** (Scheme S1; see the ESI†) which represents an isomer of dimeric germylene. The intermetallic distances in **D3** and **D5** are, however, much longer than the single Ge–Ge bond length in **1a** (Table S2†). The earlier DFT calculations¹⁵ demonstrated that the Gibbs free energy of the **D5** molecule in C₆H₆ solution exceeds that of **D1** by 1.0 kcal mol⁻¹. The computations performed in this work provide a slightly larger G difference of 3.5 kcal mol⁻¹ (Scheme S1†). Accordingly, no

long-lived **D5** species were detected experimentally. On the contrary, stable Ge(I)–Ge(I) bonded dimers were obtained with bulky amidinato and guanidinato ligands.²⁶ To reveal the reasons for such a different behaviour and to analyse the changes of the electronic structures on going from **D5** to **D3** and then to **1a** we studied these systems with MO and NBO approaches. The coordination of a C₂Me₂ molecule to **D5** (**D5** → **D3**) causes no changes in the Ge–Ge bonding situation and the nature of frontier MOs (Fig. 7 and Fig. S3; see the ESI†). The HOMO isosurface of **D5** (Fig. 7) appears to differ strongly from that of the amidinato complexes²⁶ where this orbital has a σ -bonding character relative to the Ge–Ge interaction. The HOMO of **D3** and **D5** represents mostly an antibonding combination of two Ge lone pairs. Moreover, the search of the lower-lying occupied MO in **D3** and **D5** revealed no Ge–Ge bonding orbitals except HOMO–1 with a weak positive overlap of the Ge wavefunctions. Correspondingly, the Ge–Ge distances (Table S2†) in the optimized gas-phase **D3** and **D5** structures (2.918 and 2.933 Å) appear to be much longer than those in the germanium(I) dimers stabilized by amidinato ligands²⁶ (2.679; 2.702 Å). In contrast to the latter compounds, NBO analysis reveals no Ge–Ge covalent bond in **D3** or **D5** and attributes the bonding between two monomers exclusively to the donation of the Ge lone pair (which has s character) to the

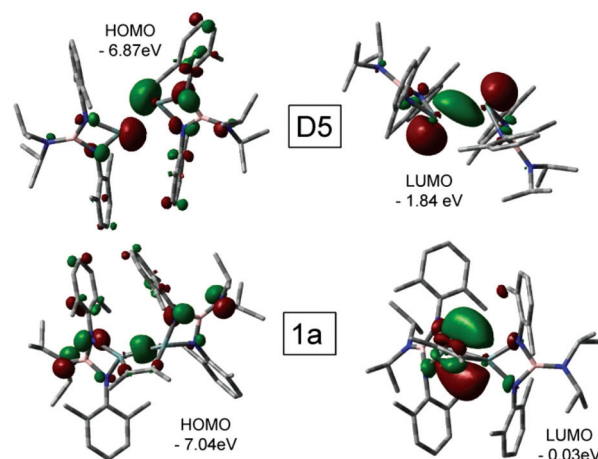


Fig. 7 Isosurfaces (isovalue 0.05) and energies of frontier MOs of **D5** (top) and **1a** (bottom). Hydrogen atoms are omitted for clarity.



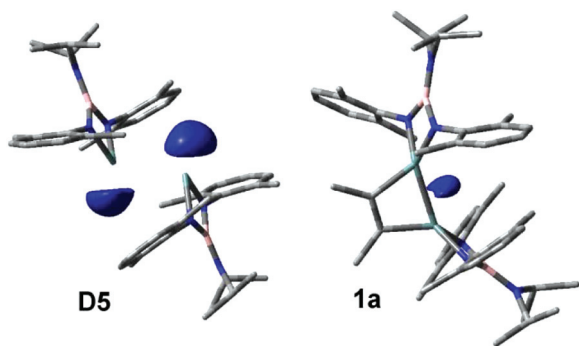


Fig. 8 Isosurfaces (isovalued 0.95 a.u.) corresponding to the contribution of the Ge atoms to the ELF functions of the **D5** (left) and **1a** (right) molecules. Hydrogen atoms are omitted for clarity.

empty p orbital of the second Ge atom. This can be explained²⁷ by the large singlet–triplet energy gap in the **M1** germylene (56.6 kcal mol^{−1}). The replacement of a carbon atom in the four-membered heterocycle of the germanium amidinato complexes with boron results, therefore, in substantial weakening of the Ge–Ge bond. On the other hand, the long Ge–Ge distance in **D3** provides additional possibilities for the alkyne → alkene transformation necessary to form the **1a** product.

On going from **D5** or **D3** to **1a**, the frontier MOs change dramatically (Fig. 7). The **1a** HOMO is responsible for the Ge–Ge σ -bonding. The NBO approach describes this interaction as a covalent bond formed by an electron pair shared by both Ge atoms. The HOMO energy decreases on going from **D5** to **1a** while the LUMO energy increases. These changes lead to an increased stability of **1a**.

The MO and NBO approaches show that the **D3** and **D5** molecules represent the case examples of digermenes where the Ge–Ge bonding is provided exclusively by donor–acceptor interactions while the **1a** species bear a Ge–Ge shared electron pair. The electron pairs can be visualised by calculation of the corresponding electron localization functions (ELF). The shared nature of the Ge electron pairs in **1a** is clearly demonstrated by the isosurface of the germanium contribution to ELF (Fig. 8). This isosurface is shifted off the Ge–Ge connecting line which illustrates the bent character of the Ge–Ge bond in **1a**. On the contrary, in **D5** the electron pairs are localized on each Ge atom (Fig. 8). The Ge–Ge electron density distribution remains practically unchanged on going from **D5** to **D3**. The MO, NBO and ELF approaches thus provide complementary data indicating that the transformation of digermene **D3** to 1,2-digermacyclobut-3-ene **1a** is accompanied by dramatic changes in the nature of the Ge–Ge interactions. This is confirmed by the QTAIM calculations (see the ESI†).

Conclusions

We have clearly demonstrated that germylene, [(i-Pr)₂NB(N-2,6-Me₂C₆H₃)₂]₂Ge, reacts with a variety of alkynes under selective formation of the corresponding substituted 1,2-digermacyclo-

but-3-enes by a formal [2 + 2 + 2] cycloaddition. Furthermore, it has been shown that only one triple bond in conjugated diynes RC≡CC≡CR enters into such cyclization reactions, whereas less sterically crowded compounds such as fc (C≡CPh)₂ (fc = 1,1'-ferrocendiyl) can react at both C≡C bonds. In particular, the interaction of fc(C≡CPh)₂ with the title germylene gives rise to an unprecedented bis(1,2-digermacyclobut-3-ene) bridged by an organometallic ferrocene fragment.

DFT calculations suggest that a plausible reaction mechanism involves weak complexes of germylene and the corresponding digermene with alkynes. The formation of a germirane appears to be unfavourable both thermodynamically and kinetically. The transformation of the digermene–alkyne complex into 1,2-digermacyclobut-3-ene as the final product is accompanied by a substantial decrease in the electronic and Gibbs free energy of the system and also by substantial changes in the Ge–Ge bonding. Further investigation will be targeted mainly at an elucidation of the reactivity of the germylene with variously substituted alkynes and diynes and other substrates containing C-heteroatom multiple bonds.

Experimental section

General considerations

Manipulations with air and moisture sensitive compounds were performed under an argon atmosphere using standard Schlenk techniques. Germylene [(i-Pr)₂NB(N-2,6-Me₂C₆H₃)₂]₂Ge,¹⁵ FcC≡CR (R = H,²⁸ Me,²⁹ Ph,³⁰ and Fc³¹), FcC≡CC≡CFc³² and fc(C≡CPh)₂³³ were prepared according to the literature procedures. All other materials were obtained from commercial suppliers and were used without any additional purification. All solvents were dried using an MD7 Pure Solv instrument (Innovative Technology, MA, USA).

¹H and ¹³C{¹H} NMR spectra were recorded on a Bruker 400 or Bruker 500 spectrometer, using a 5 mm tunable broadband probe. Chemical shifts in the ¹H and ¹³C NMR spectra were referenced to the residual solvent (C₆D₆: $\delta(^1\text{H})$ = 7.16 ppm, $\delta(^{13}\text{C})$ = 128.39 ppm). Elemental analyses were determined with a LECO-CHNS-932 analyser. Infrared spectra were recorded in the 4000–600 cm^{−1} range on a Nicolet 6700 FTIR spectrometer using a silicon ATR crystal (resolution 2 cm^{−1}). The Raman spectra of solid samples sealed in a quartz capillary were obtained on a Nicolet iS50 equipped with an iS50 Raman module (excitation laser 1064 nm, resolution 2 cm^{−1}).

Cyclic voltammetric (CV) measurements were performed with a computer-controlled potentiostat μ AUTOLAB III (Eco Chemie, the Netherlands) at room temperature (23 °C) using a standard Metrohm three-electrode cell equipped with a glassy carbon disc working electrode (2 mm diameter), platinum sheet auxiliary electrode, and a double-junction Ag/AgCl (3 M KCl) reference electrode. The compounds were dissolved in dry dichloromethane to give a solution containing ca. 1 mM of the analysed sample (or a saturated solution for poorly soluble compounds) and 0.1 M Bu₄N[PF₆] (Fluka, puriss for



electrochemistry). The solutions were purged with argon before the measurement and then kept under an argon blanket. The redox potentials (accuracy *ca.* 5 mV) were recorded relative to internal decamethylferrocene/decamethylferrocenium (added during the final scans) and then converted to the ferrocene/ferrocenium scale by subtracting 0.548 V.³⁴

General synthetic procedure

The respective alkyne was added to a light yellow solution of [(i-Pr)₂NB(N-2,6-Me₂C₆H₃)₂Ge]₂ in toluene (10 mL; hexane was used in the case of **1b**) at room temperature (r.t.) and the reaction mixture was stirred for a given time. Then, the reaction mixture was evaporated *in vacuo* and the solid residue was extracted with hexane (15 mL). The coloured extract was concentrated to one third of the original volume and then stored at a temperature (specified below) to induce crystallization of the product, which was subsequently filtered off and dried *in vacuo*.

Synthesis of [(i-Pr)₂NB(N-2,6-Me₂C₆H₃)₂Ge]₂(MeC≡CMe) (1a**).** 0.02 mL (0.3 mmol) of neat MeC≡CMe and 0.25 g (0.6 mmol) of [(i-Pr)₂NB(N-2,6-Me₂C₆H₃)₂Ge] were reacted for 24 h. After workup, the light yellow concentrated extract was stored at r.t. and compound **1a** was isolated as white crystals. Yield: 0.10 g (38%), m.p.: 210 °C with decomposition. Anal. calcd for C₄₈H₇₀B₂Ge₂N₆ (MW 898.01): C, 64.2; H, 7.9. Found: C, 64.3; H, 7.7%. ¹H NMR (500 MHz, C₆D₆): δ 0.88 (s(br), 24H, i-Pr-CH₃), 1.76 (s, 6H, C≡C-CH₃), 2.28 (s, 12H, Dmp-CH₃), 2.47 (s, 12H, Dmp-CH₃), 3.14 (h, 4H, i-Pr-CH, ³J_{H,H} = 6.9 Hz), 6.85 (t, 4H, Dmp-H₄, ³J_{H,H} = 7.4 Hz), 6.94 (d(br), 4H, Dmp-H_{3,5}), 6.99 (d(br), 4H, Dmp-H_{3,5}) ppm. ¹³C NMR (125.7 MHz, C₆D₆): δ 18.1 (s, C≡C-CH₃), 19.9 (s, Dmp-CH₃), 20.5 (s, Dmp-CH₃), 23.8 (s, i-Pr-CH₃), 46.2 (s, i-Pr-CH), 124.1 (s, Dmp-C₄), 128.7 (s, Dmp-C_{3,5}), 128.9 (s, Dmp-C_{3,5}), 135.3 (s, Dmp-C_{2,6}), 136.0 (s, Dmp-C_{2,6}), 145.3 (s, Dmp-C₁), 172.7 (s, C≡C) ppm.

Synthesis of [(i-Pr)₂NB(N-2,6-Me₂C₆H₃)₂Ge]₂(PhC≡CPh) (1b**).** 0.07 g (0.4 mmol) of solid PhC≡CPh and 0.35 g (0.8 mmol) of [(i-Pr)₂NB(N-2,6-Me₂C₆H₃)₂Ge] were reacted in hexane for 2 h. After workup the light yellow concentrated extract was stored at r.t. and compound **1b** was isolated as colorless crystals. Yield: 0.30 g (62%), m.p.: 183 °C dec. Anal. calcd for C₅₈H₇₄B₂Ge₂N₆ (1022.15): C, 68.2; H, 7.3; found: C, 68.3; H, 7.5%. ¹H NMR (500 MHz, C₆D₆): δ 0.88 (s(br), 24H, i-Pr-CH₃), 2.23 (s, 12H, Dmp-CH₃), 2.42 (s, 12H, Dmp-CH₃), 3.14 (h, 4H, i-Pr-CH, ³J_{H,H} = 6.8 Hz), 6.71 (d, 4H, Ph-H_{2,6}, ³J_{H,H} = 7.8 Hz), 6.81 (m, 2H, Ph-H₄), 6.88 (m, 8H, Dmp-H₄ + Ph-H_{3,5}), 6.95 (d(br), 4H, Dmp-H_{3,5}), 7.00 (d(br), 4H, Dmp-H_{3,5}) ppm. ¹³C NMR (125.7 MHz, C₆D₆): δ 20.5 (s, Dmp-CH₃), 20.7 (s, Dmp-CH₃), 23.8 (s, i-Pr-CH₃), 46.2 (s, i-Pr-CH), 124.2 (s, Dmp-C₄), 127.3 (s, Ph-C₄), 127.8 (s, Ph-C_{3,5}), 128.5 (s, Ph-C_{2,6}), 128.8 (s, Dmp-C_{3,5}), 129.0 (s, Dmp-C_{3,5}), 135.5 (s, Dmp-C_{2,6}), 136.2 (s, Dmp-C_{2,6}), 139.4 (s, Ph-C₁), 145.1 (s, Dmp-C₁), 176.3 (s, C≡C) ppm.

Synthesis of [(i-Pr)₂NB(N-2,6-Me₂C₆H₃)₂Ge]₂(PhC≡CH) (1c**).** 0.06 mL (0.5 mmol) of neat PhC≡CH and 0.45 g (1.1 mmol) of [(i-Pr)₂NB(N-2,6-Me₂C₆H₃)₂Ge] were stirred in toluene for 24 h. After workup, the light yellow concentrated

extract was stored at −8 °C and compound **1c** was isolated as colorless crystals. Yield: 0.28 g (55%), m.p.: 111 °C dec. Anal. calcd for C₅₂H₇₀B₂Ge₂N₆ (946.05): C, 66.0; H, 7.5; found: C, 65.9; H, 7.2%. ¹H NMR (500 MHz, C₆D₆): δ 0.87 (d, 24H, i-Pr-CH₃, ³J_{H,H} = 6.8 Hz), 2.16 (s, 6H, Dmp-CH₃), 2.37 (s, 6H, Dmp-CH₃), 2.42 (s, 6H, Dmp-CH₃), 2.44 (s, 6H, Dmp-CH₃), 3.16 (h, 4H, i-Pr-CH, ³J_{H,H} = 6.9 Hz), 6.83 (m, 6H, Dmp-H + Ph-H), 6.95 (m, 6H, Dmp-H + Ph-H), 7.03 (m, 3H, Dmp-H + Ph-H), 7.43 (m, 2H, Ph-H_{2,6}), 8.28 (s, 1H, C≡CH) ppm. ¹³C NMR (125.7 MHz, C₆D₆): δ 19.9 (s, Dmp-CH₃), 20.2 (s, Dmp-CH₃), 20.7 (s, Dmp-CH₃), 20.8 (s, Dmp-CH₃), 23.8 (s, i-Pr-CH₃), 23.9 (s, i-Pr-CH₃), 46.2 (s, i-Pr-CH), 124.2 (s, Dmp-C₄), 124.3 (s, Dmp-C₄), 128.7 (s, Ph-C), 128.8 (s, Ph-C), 128.9 (s, Dmp-C_{3,5}), 129.0 (s, Dmp-C_{3,5}), 129.4 (s, Ph-C), 135.3 (s, Dmp-C_{2,6}), 135.4 (s, Dmp-C_{2,6}), 136.1 (s, Dmp-C_{2,6}), 136.4 (s, Dmp-C_{2,6}), 138.5 (s, Ph-C₁), 144.9 (s, Dmp-C₁), 160.2 (s, C≡CH), 182.8 (s, C≡CH) ppm.

Synthesis of [(i-Pr)₂NB(N-2,6-Me₂C₆H₃)₂Ge]₂(t-BuC≡CH) (1d**).** 0.04 mL (0.3 mmol) of neat t-BuC≡CH and 0.24 g (0.6 mmol) of [(i-Pr)₂NB(N-2,6-Me₂C₆H₃)₂Ge] were stirred in toluene for 2 h. After workup, the light yellow concentrated extract was stored at −8 °C and compound **1d** was isolated in the form of colorless crystals. Yield: 0.16 g (61%), m.p.: 153 °C dec. Anal. calcd for C₅₀H₇₄B₂Ge₂N₆ (926.06): C, 64.9; H, 8.1; found: C, 64.8; H, 8.0%. ¹H NMR (500 MHz, C₆D₆): δ 0.85 (s, 9H, t-Bu-CH₃), 0.90 (d, 24H, i-Pr-CH₃, ³J_{H,H} = 6.8 Hz), 2.30 (s, 6H, Dmp-CH₃), 2.38 (s, 6H, Dmp-CH₃), 2.51 (s, 6H, Dmp-CH₃), 2.53 (s, 6H, Dmp-CH₃), 3.18 (h, 4H, i-Pr-CH, ³J_{H,H} = 6.8 Hz), 6.85 (m, 4H, Dmp-H₄), 6.97 (m, 8H, Dmp-H_{3,5}), 7.90 (s, 1H, C≡CH) ppm. ¹³C NMR (125.7 MHz, C₆D₆): δ 20.2 (s, Dmp-CH₃), 20.5 (s, Dmp-CH₃), 20.6 (s, Dmp-CH₃), 21.1 (s, Dmp-CH₃), 23.9 (s, i-Pr-CH₃), 31.0 (s, t-Bu-CH₃), 39.2 (s, t-Bu-C), 46.1 (s, i-Pr-CH), 46.5 (s, i-Pr-CH), 124.0 (s, Dmp-C₄), 124.1 (s, Dmp-C₄), 128.7 (s, Dmp-C_{3,5}), 128.9 (s, Dmp-C_{3,5}), 129.0 (s, Dmp-C_{3,5}), 129.1 (s, Dmp-C_{3,5}), 135.2 (s, Dmp-C_{2,6}), 135.5 (s, Dmp-C_{2,6}), 135.7 (s, Dmp-C_{2,6}), 136.3 (s, Dmp-C_{2,6}), 144.9 (s, Dmp-C₁), 145.5 (s, Dmp-C₁), 156.0 (s, C≡CH), 198.0 (s, C≡CH) ppm.

Synthesis of [(i-Pr)₂NB(N-2,6-Me₂C₆H₃)₂Ge]₂(CyC≡CH) (1e**).** 0.04 mL (0.4 mmol) of CyC≡CH and 0.29 g (0.7 mmol) of [(i-Pr)₂NB(N-2,6-Me₂C₆H₃)₂Ge] were stirred in toluene for 2 h. After workup, the light yellow concentrated extract was stored at −8 °C and compound **1e** was isolated as colorless crystals. Yield: 0.10 g (47%), m.p.: 183 °C. Anal. calcd for C₅₂H₇₆B₂Ge₂N₆ (952.10): C, 65.6; H, 8.1; found: C, 65.7; H, 8.2%. ¹H NMR (500 MHz, C₆D₆): δ 0.76 (m, 2H, Cy-H), 0.88 (d, 24H, i-Pr-CH₃, ³J_{H,H} = 6.9 Hz), 0.92 (m, 2H, Cy-H₄), 1.08 (m, 2H, Cy-H), 1.49 (m, 4H, Cy-H), 2.30 (s, 6H, Dmp-CH₃), 2.35 (m, 1H, Cy-H₁), 2.36 (s, 6H, Dmp-CH₃), 2.47 (s, 6H, Dmp-CH₃), 2.49 (s, 6H, Dmp-CH₃), 3.15 (m, 4H, i-Pr-CH), 6.85 (m, 4H, Dmp-H₄), 6.98 (m, 8H, Dmp-H_{3,5}), 7.85 (s, 1H, C≡CH) ppm. ¹³C NMR (125.7 MHz, C₆D₆): δ 19.9 (s, Dmp-CH₃), 20.0 (s, Dmp-CH₃), 20.3 (s, Dmp-CH₃), 20.5 (s, Dmp-CH₃), 23.9 (s, i-Pr-CH₃), 26.3 (s, Cy-C), 26.8 (s, Cy-C), 33.6 (s, Cy-C), 44.9 (s, Cy-C₁), 46.1 (s, i-Pr-CH), 46.3 (s, i-Pr-CH), 124.1 (s, Dmp-C₄), 124.2 (s, Dmp-C₄), 128.6 (s, Dmp-C_{3,5}), 128.7 (s, Dmp-C_{3,5}),



128.8 (s, Dmp-C3,5), 129.0 (s, Dmp-C3,5), 135.4 (s, Dmp-C2,6), 135.5 (s, Dmp-C2,6), 135.7 (s, Dmp-C2,6), 136.5 (s, Dmp-C2,6), 145.0 (s, Dmp-C1), 145.3 (s, Dmp-C1), 157.6 (s, C=CH), 192.8 (s, C=CH) ppm.

Synthesis of $\{[(i\text{-Pr})_2\text{NB}(N\text{-}2,6\text{-Me}_2\text{C}_6\text{H}_3)_2]\text{Ge}\}_2(\text{FcC}\equiv\text{CH})$ (2a). 0.06 g (0.3 mmol) of solid $\text{FcC}\equiv\text{CH}$ and 0.22 g (0.5 mmol) of $[(i\text{-Pr})_2\text{NB}(N\text{-}2,6\text{-Me}_2\text{C}_6\text{H}_3)_2]\text{Ge}$ were stirred in toluene for 24 h. After workup, the dark red concentrated extract was stored at 4 °C and compound **2a** was isolated as dark red crystals. Yield: 0.15 g (55%), m.p.: 196 °C. Anal. calcd for $\text{C}_{56}\text{H}_{74}\text{B}_2\text{FeGe}_2\text{N}_6$ (1053.97): C, 63.8; H, 7.1; found: C, 63.6; H, 7.3%. ^1H NMR (500 MHz, C_6D_6): δ 0.88 (m, 24H, *i*-Pr-CH₃), 2.33 (s, 6H, Dmp-CH₃), 2.35 (s, 6H, Dmp-CH₃), 2.49 (s, 6H, Dmp-CH₃), 2.53 (s, 6H, Dmp-CH₃), 3.17 (h, 4H, *i*-Pr-CH, $^3J_{\text{H,H}} = 6.8$ Hz), 3.60 (s, 5H, Cp-H), 4.06 (t, 2H, C=CCp-H, $^3J_{\text{H,H}} = 1.9$ Hz), 4.58 (t, 2H, C=CCp-H, $^3J_{\text{H,H}} = 1.9$ Hz), 6.83 (m, 4H, Dmp-H4), 6.93 (m, 4H, Dmp-H3,5), 7.00 (m, 4H, Dmp-H3,5), 8.10 (s, 1H, C=CH) ppm. ^{13}C NMR (125.7 MHz, C_6D_6): δ 19.8 (s, Dmp-CH₃), 20.4 (s, Dmp-CH₃), 20.4 (s, Dmp-CH₃), 21.2 (s, Dmp-CH₃), 23.9 (s, *i*-Pr-CH₃), 24.1 (s, *i*-Pr-CH₃), 46.2 (s, *i*-Pr-CH), 46.3 (s, *i*-Pr-CH), 70.4 (s, C=CCp-C), 71.1 (s, Cp-C), 71.2 (s, C=CCp-C), 80.9 (s, C=CCp-C1), 124.3 (s, Dmp-C4), 124.4 (s, Dmp-C4), 128.7 (s, Dmp-C3,5), 128.8 (overlap of two signals, Dmp-C3,5), 128.9 (s, Dmp-C3,5), 135.6 (s, Dmp-C2,6), 135.7 (s, Dmp-C2,6), 136.3 (s, Dmp-C2,6), 136.5 (s, Dmp-C2,6), 144.9 (s, Dmp-C1), 145.3 (s, Dmp-C1), 155.8 (s, C=CH), 181.0 (s, C=CH) ppm.

Synthesis of $\{[(i\text{-Pr})_2\text{NB}(N\text{-}2,6\text{-Me}_2\text{C}_6\text{H}_3)_2]\text{Ge}\}_2(\text{FcC}\equiv\text{CMe})$ (2b). 0.05 g (0.2 mmol) of $\text{FcC}\equiv\text{CMe}$ and 0.20 g (0.5 mmol) of $[(i\text{-Pr})_2\text{NB}(N\text{-}2,6\text{-Me}_2\text{C}_6\text{H}_3)_2]\text{Ge}$ were reacted in toluene for 24 h. After workup, the dark red concentrated extract was stored at 4 °C and compound **2b** was isolated as dark red crystals. Yield: 0.08 g (31%), m.p.: 233 °C. Anal. calcd for $\text{C}_{57}\text{H}_{76}\text{B}_2\text{FeGe}_2\text{N}_6$ (1068.00): C, 64.1; H, 7.2; found: C, 64.4; H, 7.3%. ^1H NMR (500 MHz, C_6D_6): δ 0.91 (m, 24H, *i*-Pr-CH₃), 2.21 (s, 3H, C=C-CH₃), 2.33 (s, 6H, Dmp-CH₃), 2.39 (s, 6H, Dmp-CH₃), 2.54 (s, 12H, Dmp-CH₃), 3.20 (m, 4H, *i*-Pr-CH), 3.69 (s, 5H, Cp-H), 4.08 (s, 2H, C=CCp-H), 4.71 (s, 2H, C=CCp-H), 6.80 (m, 2H, Dmp-H4), 6.86 (m, 2H, Dmp-H4), 6.93 (m, 4H, Dmp-H3,5), 6.97 (d, 2H, Dmp-H3,5, $^3J_{\text{H,H}} = 7.4$ Hz), 7.03 (d, 2H, Dmp-H3,5, $^3J_{\text{H,H}} = 7.6$ Hz) ppm. ^{13}C NMR (125.7 MHz, C_6D_6): δ 20.3 (s, Dmp-CH₃), 20.7 (s, C=C-CH₃), 20.8 (s, Dmp-CH₃), 21.6 (s, Dmp-CH₃), 24.0 (s, *i*-Pr-CH₃), 24.1 (s, *i*-Pr-CH₃), 46.3 (s, *i*-Pr-CH), 69.9 (s, C=CCp-C), 70.4 (s, Cp-C), 71.8 (s, C=CCp-C), 81.3 (s, C=CCp-C1), 124.0 (s, Dmp-C4), 124.1 (s, Dmp-C4), 128.7 (s, Dmp-C3,5), 128.9 (s, Dmp-C3,5), 129.0 (s, Dmp-C3,5), 135.1 (s, Dmp-C2,6), 135.6 (s, Dmp-C2,6), 136.1 (s, Dmp-C2,6), 136.2 (s, Dmp-C2,6), 145.1 (s, Dmp-C1), 145.4 (s, Dmp-C1), 168.3 (s, C=C), 170.9 (s, C=C) ppm.

Synthesis of $\{[(i\text{-Pr})_2\text{NB}(N\text{-}2,6\text{-Me}_2\text{C}_6\text{H}_3)_2]\text{Ge}\}_2(\text{FcC}\equiv\text{CPh})$ (2c). 0.08 g (0.3 mmol) of solid $\text{FcC}\equiv\text{CPh}$ and 0.23 g (0.5 mmol) of $[(i\text{-Pr})_2\text{NB}(N\text{-}2,6\text{-Me}_2\text{C}_6\text{H}_3)_2]\text{Ge}$ were stirred in toluene for 24 h. After workup, the dark red concentrated extract was stored at 4 °C and compound **2c** was isolated as dark red crystals. Yield: 0.18 g (59%), m.p.: 237 °C. Anal. calcd for $\text{C}_{62}\text{H}_{78}\text{B}_2\text{FeGe}_2\text{N}_6$ (1130.07): C, 65.1; H, 7.0; found: C, 65.2;

H, 7.1%. ^1H NMR (500 MHz, C_6D_6): δ 0.77 (s(br), 6H, *i*-Pr-CH₃), 0.96 (s(br), 18H, *i*-Pr-CH₃), 2.27 (s, 6H, Dmp-CH₃), 2.35 (s, 6H, Dmp-CH₃), 2.41 (s, 6H, Dmp-CH₃), 2.73 (s, 6H, Dmp-CH₃), 3.12 (h, 2H, *i*-Pr-CH, $^3J_{\text{H,H}} = 6.8$ Hz), 3.28 (h, 2H, *i*-Pr-CH, $^3J_{\text{H,H}} = 6.8$ Hz), 3.64 (s, 5H, Cp-H), 3.88 (t, 2H, C=CCp-H, $^3J_{\text{H,H}} = 1.9$ Hz), 4.35 (t, 2H, C=CCp-H, $^3J_{\text{H,H}} = 1.9$ Hz), 6.58 (m, 2H, Ph-H3,5), 6.86 (m, 4H, Dmp-H4), 6.99 (m, 9H, Dmp-H3,5 + Ph-H2,6 + Ph-H4), 7.06 (m, 2H, Dmp-H3,5) ppm. ^{13}C NMR (125.7 MHz, C_6D_6): δ 20.8 (s, Dmp-CH₃), 21.1 (s, Dmp-CH₃), 21.8 (s, Dmp-CH₃), 23.4 (s, Dmp-CH₃), 24.1 (s(br), *i*-Pr-CH₃), 46.3 (s, *i*-Pr-CH), 46.5 (s, *i*-Pr-CH), 70.3 (s, C=CCp-C), 70.7 (s, Cp-C), 71.9 (s, C=CCp-C), 80.5 (s, C=CCp-C1), 124.0 (s, Dmp-C4), 126.9 (s, Ph-C4), 127.0 (s, Ph-C3,5), 128.8 (s, Dmp-C3,5), 128.9 (s, Dmp-C3,5), 129.0 (s, Dmp-C3,5), 129.0 (s, Dmp-C3,5), 129.2 (s, Ph-C2,6), 135.2 (s, Dmp-C2,6), 135.3 (s, Dmp-C2,6), 135.5 (s, Dmp-C2,6), 136.5 (s, Dmp-C2,6), 142.1 (s, Ph-C1), 145.2 (s, Dmp-C1), 145.6 (s, Dmp-C1), 169.8 (s, C=C), 171.8 (s, C=C) ppm.

Synthesis of $\{[(i\text{-Pr})_2\text{NB}(N\text{-}2,6\text{-Me}_2\text{C}_6\text{H}_3)_2]\text{Ge}\}_2(\text{FcC}\equiv\text{CFc})$ (2d). 0.10 g (0.3 mmol) of $\text{FcC}\equiv\text{CFc}$ and 0.22 g (0.5 mmol) of $[(i\text{-Pr})_2\text{NB}(N\text{-}2,6\text{-Me}_2\text{C}_6\text{H}_3)_2]\text{Ge}$ were stirred in toluene for 24 h. After workup, the red concentrated extract was stored at r.t. and compound **2b** was isolated as red crystals. Yield: 0.11 g (34%), m.p.: 211 °C. Anal. calcd for $\text{C}_{66}\text{H}_{82}\text{B}_2\text{Fe}_2\text{Ge}_2\text{N}_6$ (1237.99): C, 64.0; H, 6.7; found: C, 64.2; H, 6.6%. ^1H NMR (500 MHz, C_6D_6): δ 0.89 (s(br), 24H, *i*-Pr-CH₃), 2.40 (s(br), 24H, Dmp-CH₃), 3.18 (h, 4H, *i*-Pr-CH, $^3J_{\text{H,H}} = 6.9$ Hz), 3.79 (s, 10H, Cp-H), 4.31 (s, 2H, C=CCp-H), 5.68 (s, 2H, C=CCp-H), 6.86 (s(br), 4H, Dmp-H4), 7.00 (s(br), 4H, Dmp-H3,5), 6.86 (d(br), 4H, Dmp-H3,5, $^3J_{\text{H,H}} = 6.9$ Hz) ppm. ^{13}C NMR (125.7 MHz, C_6D_6): δ 21.3 (s(br), Dmp-CH₃), 21.8 (s(br), Dmp-CH₃), 24.1 (s(br), *i*-Pr-CH₃), 46.3 (s, *i*-Pr-CH), 70.3 (s(br), C=CCp-C), 70.9 (s, Cp-C), 72.9 (s(br), C=CCp-C), 80.9 (s, C=CCp-C1), 124.3 (s, Dmp-C4), 128.8 (s, Dmp-C3,5), 129.1 (s, Dmp-C3,5), 135.8 (s, Dmp-C2,6), 136.9 (s, Dmp-C1), 163.7 (s, C=C) ppm.

Synthesis of $\{[(i\text{-Pr})_2\text{NB}(N\text{-}2,6\text{-Me}_2\text{C}_6\text{H}_3)_2]\text{Ge}\}_2(\text{PhC}\equiv\text{CC}\equiv\text{CPh})$ (3a). 0.07 g (0.3 mmol) of $\text{PhC}\equiv\text{CC}\equiv\text{CPh}$ and 0.27 g (0.7 mmol) of $[(i\text{-Pr})_2\text{NB}(N\text{-}2,6\text{-Me}_2\text{C}_6\text{H}_3)_2]\text{Ge}$ were stirred in toluene for 5 d. After workup, the yellow concentrated extract was stored at r.t. and compound **3a** was isolated as yellow crystals. Yield: 0.17 g (51%), m.p.: 176 °C. Anal. calcd for $\text{C}_{60}\text{H}_{74}\text{B}_2\text{Ge}_2\text{N}_6$ (1046.17): C, 68.9; H, 7.1; found: C, 69.0; H, 7.1%. ^1H NMR (500 MHz, C_6D_6): δ 0.89 (m, 24H, *i*-Pr-CH₃), 2.15 (s, 6H, Dmp-CH₃), 2.39 (s, 6H, Dmp-CH₃), 2.46 (s, 6H, Dmp-CH₃), 2.72 (s, 6H, Dmp-CH₃), 3.18 (m, 4H, *i*-Pr-CH), 6.83 (m, 6H, Dmp-H + Ph-H), 7.00 (m, 10H, Dmp-H + Ph-H), 7.10 (m, 2H, Dmp-H + Ph-H), 7.41 (d, 2H, Ph-H2,6, $^3J_{\text{H,H}} = 7.7$ Hz), 7.84 (d, 2H, Ph-H2,6, $^3J_{\text{H,H}} = 7.7$ Hz) ppm. ^{13}C NMR (125.7 MHz, C_6D_6): δ 20.2 (s, Dmp-CH₃), 20.6 (s, Dmp-CH₃), 20.8 (s, Dmp-CH₃), 20.9 (s, Dmp-CH₃), 23.9 (s, *i*-Pr-CH₃), 23.9 (s, *i*-Pr-CH₃), 46.2 (s, *i*-Pr-CH), 46.3 (s, *i*-Pr-CH), 88.4 (s, C=C-Ph), 108.7 (s, C=C-C=C), 124.3 (s, Dmp-C4), 124.5 (s, Dmp-C4), 128.6 (s, Ph-C4), 128.7 (s, Ph-C3,5), 128.8 (s, Ph-C2,6), 128.9 (s, Dmp-C3,5), 129.1 (overlap of two signals, Dmp-C3,5 + Ph-C), 129.3 (overlap of two signals, Dmp-C3,5 + Ph-C), 129.4 (s, Dmp-C3,5), 132.1 (s, Ph-C2,6), 135.5 (s, Dmp-C2,6),



135.9 (s, Dmp-C2,6), 136.0 (s, Dmp-C2,6), 136.0 (s, Dmp-C2,6), 138.7 (s, Ph-C1), 144.6 (s, Dmp-C1), 144.7 (s, Dmp-C1), 153.1 (s, C=C-Ph), 180.4 (s, C=C-C≡C) ppm.

Synthesis of $\{[(i\text{-Pr})_2\text{NB}(N\text{-}2,6\text{-Me}_2\text{C}_6\text{H}_3)_2]\text{Ge}\}_2(t\text{-BuC}\equiv\text{CC}\equiv\text{Ct-Bu})$ (3b**).** 0.05 g (0.3 mmol) of $t\text{-BuC}\equiv\text{CC}\equiv\text{Ct-Bu}$ and 0.23 g (0.6 mmol) of $[(i\text{-Pr})_2\text{NB}(N\text{-}2,6\text{-Me}_2\text{C}_6\text{H}_3)_2]\text{Ge}$ were stirred in toluene for 5 d. After workup, the yellow concentrated extract was stored at r.t. and compound **3b** was isolated as yellow crystals. Yield: 0.11 g (38%), m.p.: 202 °C. Anal. calcd for $\text{C}_{56}\text{H}_{82}\text{B}_2\text{Ge}_2\text{N}_6$ (1006.19): C, 66.9; H, 8.2; found: C, 67.0; H, 8.1%. ^1H NMR (500 MHz, C_6D_6): δ 0.95 (d, 24H, $i\text{-Pr-CH}_3$, $^3J_{\text{H,H}} = 6.8$ Hz), 1.17 (s, 9H, $t\text{-Bu-CH}_3$), 1.19 (s, 9H, $t\text{-Bu-CH}_3$), 2.27 (s, 6H, Dmp- CH_3), 2.39 (s, 6H, Dmp- CH_3), 2.55 (s, 6H, Dmp- CH_3), 2.74 (s, 6H, Dmp- CH_3), 3.21 (h, 4H, $i\text{-Pr-CH}$, $^3J_{\text{H,H}} = 6.8$ Hz), 6.81 (t, 2H, Dmp- H_4 , $^3J_{\text{H,H}} = 7.4$ Hz), 6.87 (m, 4H, Dmp- $\text{H}_{3,5} + \text{Dmp-}\text{H}_4$), 6.98 (m, 4H, Dmp- $\text{H}_{3,5}$), 7.06 (d(br), 2H, Dmp- $\text{H}_{3,5}$) ppm. ^{13}C NMR (125.7 MHz, C_6D_6): δ 20.7 (s, Dmp- CH_3), 21.0 (s, Dmp- CH_3), 21.4 (s, Dmp- CH_3), 21.7 (s, Dmp- CH_3), 23.9 (s, $i\text{-Pr-CH}_3$), 30.3 (s, $t\text{-Bu-CH}_3$), 30.8 (s, $t\text{-Bu-CH}_3$), 40.0 (s, $t\text{-Bu-C}$), 46.2 (s, $i\text{-Pr-CH}$), 46.6 (s, $i\text{-Pr-CH}$), 78.2 (s, C≡C- $t\text{-Bu}$), 120.4 (s, C≡C-C≡C), 123.9 (s, Dmp-C4), 124.1 (s, Dmp-C4), 128.7 (s, Dmp-C3,5), 128.8 (s, Dmp-C3,5), 129.1 (s, Dmp-C3,5), 129.2 (s, Dmp-C3,5), 134.8 (s, Dmp-C2,6), 135.1 (s, Dmp-C2,6), 135.7 (s, Dmp-C2,6), 135.9 (s, Dmp-C2,6), 144.8 (s, Dmp-C1), 145.3 (s, Dmp-C1), 154.3 (s, C=C- $t\text{-Bu}$), 193.6 (s, C=C-C≡C) ppm.

Synthesis of $\{[(i\text{-Pr})_2\text{NB}(N\text{-}2,6\text{-Me}_2\text{C}_6\text{H}_3)_2]\text{Ge}\}_2(\text{FcC}\equiv\text{CC}\equiv\text{CFc})$ (3c**).** 0.15 g (0.4 mmol) of $\text{FcC}\equiv\text{CC}\equiv\text{CFc}$ and 0.30 g (0.7 mmol) of $[(i\text{-Pr})_2\text{NB}(N\text{-}2,6\text{-Me}_2\text{C}_6\text{H}_3)_2]\text{Ge}$ were reacted in toluene for 5 d. After workup, the dark red concentrated extract was stored at r.t. and compound **3c** was isolated as dark red crystals. Yield: 0.35 g (77%), m.p.: 212 °C. Anal. calcd for $\text{C}_{68}\text{H}_{82}\text{B}_2\text{Fe}_2\text{Ge}_2\text{N}_6$ (1262.01): C, 64.7; H, 6.6; found: C, 64.9; H, 6.7%. ^1H NMR (500 MHz, C_6D_6): δ 0.89 (d, 12H, $i\text{-Pr-CH}_3$, $^3J_{\text{H,H}} = 6.5$ Hz), 0.96 (d, 12H, $i\text{-Pr-CH}_3$, $^3J_{\text{H,H}} = 6.5$ Hz), 2.35 (s, 6H, Dmp- CH_3), 2.38 (s, 6H, Dmp- CH_3), 2.59 (s, 6H, Dmp- CH_3), 2.81 (s, 6H, Dmp- CH_3), 3.22 (m, 4H, $i\text{-Pr-CH}$), 3.87 (s, 5H, Cp- H), 4.04 (m, 2H, subst.-Cp- H), 4.17 (s, 5H, Cp- H), 4.22 (m, 2H, subst.-Cp- H), 4.45 (m, 2H, subst.-Cp- H), 5.39 (m, 2H, subst.-Cp- H), 6.80 (t, 2H, Dmp- H_4 , $^3J_{\text{H,H}} = 7.5$ Hz), 6.86 (t, 2H, Dmp- H_4 , $^3J_{\text{H,H}} = 7.5$ Hz), 6.91 (d, 2H, Dmp- $\text{H}_{3,5}$, $^3J_{\text{H,H}} = 7.0$ Hz), 6.93 (d, 2H, Dmp- $\text{H}_{3,5}$, $^3J_{\text{H,H}} = 7.5$ Hz), 6.99 (d, 2H, Dmp- $\text{H}_{3,5}$, $^3J_{\text{H,H}} = 7.0$ Hz), 7.06 (d, 2H, Dmp- $\text{H}_{3,5}$, $^3J_{\text{H,H}} = 7.0$ Hz) ppm. ^{13}C NMR (125.7 MHz, C_6D_6): δ 20.1 (s, Dmp- CH_3), 20.6 (s, Dmp- CH_3), 21.2 (s, Dmp- CH_3), 21.5 (s, Dmp- CH_3), 24.0 (s, $i\text{-Pr-CH}_3$), 24.1 (s, $i\text{-Pr-CH}_3$), 46.3 (s, $i\text{-Pr-CH}$), 46.4 (s, $i\text{-Pr-CH}$), 66.8 (s, Cp-C1), 70.2 (s, subst.-Cp-C), 70.6 (s, subst.-Cp-C), 70.7 (s, Cp-C), 71.2 (s, Cp-C), 71.5 (s, subst.-Cp-C), 71.9 (s, subst.-Cp-C), 81.8 (s, Cp-C1), 87.2 (s, C≡C-Fc), 110.4 (s, C≡C-C≡C), 124.4 (overlap of two signals, Dmp-C4), 128.8 (s, Dmp-C3,5), 128.9 (s, Dmp-C3,5), 129.0 (s, Dmp-C3,5), 129.0 (s, Dmp-C3,5), 135.7 (s, Dmp-C2,6), 136.1 (s, Dmp-C2,6), 136.1 (s, Dmp-C2,6), 136.2 (s, Dmp-C2,6), 144.8 (s, Dmp-C1), 145.1 (s, Dmp-C1), 148.1 (s, C=C-Fc), 177.2 (s, C=C-C≡C) ppm.

Synthesis of $\{[(i\text{-Pr})_2\text{NB}(N\text{-}2,6\text{-Me}_2\text{C}_6\text{H}_3)_2]\text{Ge}\}_2\mu\text{-}[1,1'-(\text{PhC}\equiv\text{C})_2\text{fc}]\{[(i\text{-Pr})_2\text{NB}(N\text{-}2,6\text{-Me}_2\text{C}_6\text{H}_3)_2]\text{Ge}\}_2$ (4**).** 0.05 g

(0.1 mmol) of $\text{fc}(\text{C}\equiv\text{CPh})_2$ and 0.22 g (0.5 mmol) of $[(i\text{-Pr})_2\text{NB}(N\text{-}2,6\text{-Me}_2\text{C}_6\text{H}_3)_2]\text{Ge}$ were reacted in toluene for 7 d. After evaporation of the reaction mixture *in vacuo*, the orange solid was washed by 50 ml of hexane and compound **4** was isolated as orange powder. Yield: 0.12 g (45%), m.p.: 240 °C. Anal. calcd for $\text{C}_{114}\text{H}_{146}\text{B}_4\text{FeGe}_4\text{N}_{12}$ (2074.11): C, 66.0; H, 7.1; found: C, 65.9; H, 7.0%. ^1H NMR (500 MHz, C_6D_6): δ 0.75 (s(br), 36H, $i\text{-Pr-CH}_3$), 0.95 (s(br), 12H, $i\text{-Pr-CH}_3$), 2.22 (s, 12H, Dmp- CH_3), 2.31 (s, 12H, Dmp- CH_3), 2.36 (s, 12H, Dmp- CH_3), 2.59 (s, 12H, Dmp- CH_3), 3.09 (h, 4H, $i\text{-Pr-CH}$, $^3J_{\text{H,H}} = 6.8$ Hz), 3.25 (h, 4H, $i\text{-Pr-CH}$, $^3J_{\text{H,H}} = 6.8$ Hz), 3.37 (s, 4H, Cp- H), 4.30 (s, 4H, Cp- H), 6.50 (m, 4H, Dmp- $\text{H} + \text{Ph-}\text{H}$), 6.83 (m, 8H, Dmp- $\text{H} + \text{Ph-}\text{H}$), 6.91 (m, 8H, Dmp- $\text{H} + \text{Ph-}\text{H}$), 6.96 (m, 8H, Dmp- $\text{H} + \text{Ph-}\text{H}$), 7.04 (m, 6H, Dmp- $\text{H} + \text{Ph-}\text{H}$) ppm. ^{13}C NMR (125.7 MHz, C_6D_6): δ 20.9 (s, Dmp- CH_3), 21.0 (s, Dmp- CH_3), 21.1 (s, Dmp- CH_3), 21.6 (s, Dmp- CH_3), 24.1 (s(br), $i\text{-Pr-CH}_3$), 46.2 (s, $i\text{-Pr-CH}$), 46.4 (s, $i\text{-Pr-CH}$), 73.5 (s, Cp-C), 74.7 (s, Cp-C), 79.2 (s, Cp-C1), 124.0 (overlap of two signals, Dmp-C4), 126.8 (s, Ph-C3,5), 126.9 (s, Ph-C4), 128.9 (overlap of two signals, Dmp-C3,5 + Ph-C2,6), 129.0 (s, Dmp-C3,5), 129.1 (s, Dmp-C3,5), 129.1 (s, Dmp-C3,5), 135.2 (s, Dmp-C2,6), 135.2 (s, Dmp-C2,6), 135.5 (s, Dmp-C2,6), 136.3 (s, Dmp-C2,6), 141.8 (s, Ph-C1), 145.0 (s, Dmp-C1), 145.4 (s, Dmp-C1), 169.9 (s, C=C), 170.6 (s, C=C) ppm.

DFT calculations

The mechanism of the reaction between germylene, $[(i\text{-Pr})_2\text{NB}(N\text{-}2,6\text{-Me}_2\text{C}_6\text{H}_3)_2]\text{Ge}$, and dimethylacetylene was modeled by the DFT method employing the Gaussian09³⁵ package. All the calculations were performed at the M062X/DGDZVP level. M062X is a hybrid meta-GGA exchange–correlation functional recommended³⁶ for the studies of main-group thermochemistry, kinetics and non-covalent interactions. The double- ζ -plus-polarization DGDZVP basis set³⁷ was shown to be a good choice when describing the electronic structures of germylenes.³⁸ The molecular geometries were fully optimized in closed-shell singlet states, the experimental X-ray structures being used as the starting points for the germylene dimer **D1** and the final complex **1a**. Harmonic vibrational frequencies were computed to confirm the convergence to a minimum or a first-order saddle point on the potential energy surface and to estimate Gibbs energies. The electronic energies of the optimized geometries were taken for the reaction ΔE calculations. For transition states, the quadratic synchronous transit (QST3) method³⁹ was applied. Solvent effects in benzene were evaluated by means of the polarizable continuum model (PCM)⁴⁰ at the same level of DFT. The PCM and gas-phase optimized geometries were very similar. Gibbs energies in solution (G_{sol}) were calculated on the basis of the gas-phase values G_{gas} and electronic energy changes on solvation as follows:⁴¹

$$G_{\text{sol}} = G_{\text{gas}} + (E_{\text{sol}} - E_{\text{gas}}).$$

For transition states in solution the gas-phase optimized geometries were used. The basis set superposition errors (BSSE) were taken into account by the counterpoise corrections.⁴²



The DFT calculations of selected species were accompanied by NBO analysis⁴³ using NBO Version 3.1 incorporated into the Gaussian package. The QTAIM⁴⁴ computations were carried out with the AIMALL program suite.⁴⁵ To study the ELF topology, the Multiwfn code⁴⁶ was used.

X-ray crystallography

The X-ray data for colorless crystals of **1a**, **1b**, **1c**, **2a**, **2c**, **3a** and **3b** were obtained at 150(2) K using an Oxford Cryostream low-temperature device and a Nonius Kappa CCD diffractometer with Mo/K α radiation ($\lambda = 0.71073$ Å) using a graphite monochromator and the ϕ and χ scan modes. Data reductions were performed with DENZO-SMN.⁴⁷ The absorption was corrected by integration methods⁴⁸ or performed analytically using SADABS software⁴⁹ for **3b** and **4**. Structures were solved by direct methods (SIR92)⁵⁰ and refined by the full matrix least-squares method based on F^2 (SHELXL97).⁵¹

Full-sets of the diffraction data for **4** were collected at 150(2) K with a Bruker D8-Venture diffractometer equipped with Mo (Mo/K α radiation; $\lambda = 0.71073$ Å) microfocus X-ray (I μ S) sources, a Photon CMOS detector and an Oxford Cryosystems cooling device. The frames were integrated with the Bruker SAINT software package using a narrow-frame algorithm. The data were corrected for absorption effects using the multi-scan method (SADABS). The structures were solved and refined using XT-version 2014/5 and SHELXL-2014/7 software implemented in an APEX3 v2016.5-0 (Bruker AXS) system.⁵²

Hydrogen atoms were mostly localized on a difference Fourier map. However to ensure uniformity of treatment of the crystal structures, all hydrogen were recalculated into their idealized positions (riding model) and assigned temperature factors $U_{\text{iso}}(\text{H}) = 1.2U_{\text{eq}}$ (pivotal atom) or of $1.5U_{\text{eq}}$ (methyl). Hydrogen atoms in methyl, methylene, methine, and vinylidene moieties and hydrogen atoms in aromatic rings were placed in their theoretical positions with C–H distances of 0.96, 0.97, 0.98, 0.93 and 0.93 Å (0.86 or 0.82 Å for N–H or O–H bonds).

The structure of **1a** contains four positionally disordered isopropyl groups and one 2,6-dimethyl phenyl group which were split into two positions with approximate occupancy 1 : 1. These disorders have been modeled according to the positions of the residual electron density maxima on the Fourier electron density maps and treated by the standard SHELXL instructions.⁵² The structure of **1c** contains four positionally disordered isopropyl groups, which were treated by the SAME, RIGU and EADP instructions. A disorder was observed also in the structure of **3a**, which was dealt with similarly. In this case, a disordered isopropyl groups was split into two positions with occupancy of 1 : 1. In the structure of **3b**, the same procedure was used for modelling disorder at one of the *t*-butyl groups (occupancies 55 : 45).

Residual electron maximum and small cavities were observed within the unit cell of **1b** probably originating from an unsolved disorder. PLATON/SQUEZZE⁵³ was used to mask the cavity. A potential solvent volume of 224 Å³ was found with 16 electrons per unit cell that were located in the void which

does not respond to any of the solvents used. On the other hand, the structure of **2c** contained residual electron maxima attributable to disordered hexane. PLATON/SQUEZZE⁵³ was used to correct the data for the presence of this disordered solvent. A potential solvent volume of 559 Å³ was found with 109 electrons per unit cell worth scattering located in the void. The amount of solvent was calculated to be two molecules of hexane per unit cell which results in 100 electrons per unit cell. A similar problem was encountered in the case of compound **4**. Even in this case PLATON/SQUEZZE⁵³ procedure was used to correct the data. A potential solvent volume of 566 Å³ was found with 200 electrons per unit cell, which corresponds to six molecules of toluene.

Crystallographic data for structural analysis have been deposited with the Cambridge Crystallographic Data Centre under CCDC no. 1533462–1533469..

Conflicts of interest

There are no conflicts to declare.

Acknowledgements

The authors would like to thank the Grant Agency of the Czech Republic (P207/17-10377S) for financial support. The theoretical part of this work was supported by the Russian Foundation for Basic Research (Project 16-03-01109).

Notes and references

- For early examples see: (a) P. J. Davidson and M. F. Lappert, *J. Chem. Soc., Chem. Commun.*, 1973, 317; (b) P. J. Davidson, A. Hudson, M. F. Lappert and P. W. Lednor, *J. Chem. Soc., Chem. Commun.*, 1973, 829–830; (c) D. H. Harris and M. F. Lappert, *J. Chem. Soc., Chem. Commun.*, 1974, 895–896; (d) P. J. Davidson, D. H. Harris and M. F. Lappert, *J. Chem. Soc., Dalton Trans.*, 1976, 2268–2274; (e) M. F. Lappert and P. P. Power, *Adv. Chem. Res.*, 1976, 157, 70–81; (f) M. J. S. Gynane, D. H. Harris, M. F. Lappert, P. P. Power, P. Riviere and M. Riviere-Baudet, *J. Chem. Soc., Dalton Trans.*, 1977, 2004–2009; (g) M. F. Lappert, P. P. Power, M. J. Slade, L. Hedberg, K. Hedberg and V. Schomaker, *J. Chem. Soc., Chem. Commun.*, 1979, 369–370; (h) M. F. Lappert, *Adv. Chem. Res.*, 1976, 150, 256; (i) D. E. Goldberg, D. H. Harris, M. F. Lappert and K. M. Thomas, *J. Chem. Soc., Chem. Commun.*, 1976, 261–262.
- For selected reviews see: (a) M. Asay, C. Jones and M. Driess, *Chem. Rev.*, 2011, 221, 354–396, and references cited therein; (b) V. Y. Lee and A. Sekiguchi, *Organometallic Compounds of Low-Coordinated Si, Ge, Sn, and Pb*, Wiley, Chichester, U.K., 2010; (c) S. Nagendran and H. W. Roesky, *Organometallics*, 2007, 27, 457–492; (d) W. P. Leung,



- K. W. Kan and K. H. Chong, *Coord. Chem. Rev.*, 2007, **251**, 2253–2265.
- 3 For recent examples see: (a) T. J. Handlington, M. Hermann, G. Frenking and C. Jones, *J. Am. Chem. Soc.*, 2014, **136**, 3028–3031; (b) J. W. Dube, Z. D. Brown, C. A. Caputo, P. P. Power and P. J. Ragoon, *Chem. Commun.*, 2014, **50**, 1944–1946; (c) Z. D. Brown and P. P. Power, *Inorg. Chem.*, 2013, **52**, 6248–6259; (d) Z. D. Brown, P. Vaskko, J. D. Erickson, J. C. Fetting, H. M. Tuononen and P. P. Power, *J. Am. Chem. Soc.*, 2013, **135**, 6257–6261; (e) J. W. Dube, C. M. E. Graham, C. L. B. Macdonald, Z. D. Brown, P. P. Power and P. J. Ragoon, *Chem. – Eur. J.*, 2014, **20**, 6739–6744; (f) Z. D. Brown, J. D. Erickson, J. C. Fetting and P. P. Power, *Organometallics*, 2013, **32**, 617–622; (g) G. W. Tan, W. Y. Wang, B. Blom and M. Driess, *Dalton Trans.*, 2014, **43**, 6006–6011; (h) W. Wang, S. Inoue, S. Yao and M. Driess, *Organometallics*, 2011, **30**, 6490–6494; (i) Y. Peng, J. D. Guo, B. D. Ellis, Z. Zhu, J. C. Fetting, S. Nagase and P. P. Power, *J. Am. Chem. Soc.*, 2009, **131**, 16272–16282; (j) Y. Peng, B. D. Ellis, X. Wang and P. P. Power, *J. Am. Chem. Soc.*, 2008, **130**, 12268–12269.
- 4 For examples see: (a) M. Weidenbruch, *Eur. J. Inorg. Chem.*, 1999, 373–381; (b) Y. Mizuhata, T. Sasamori and N. Tokito, *Chem. Rev.*, 2009, **109**, 3479–3511; (c) J. A. Hardwick and K. M. Baines, *Angew. Chem., Int. Ed.*, 2015, **54**, 6600–6603; (d) J. Hlina, J. Baumgartner, C. Marschner, L. Albers, T. Müller and V. V. Jouikov, *Chem. – Eur. J.*, 2014, **20**, 9357–9366; (e) K. W. Klinkhammer, in *The Chemistry of Organic Germanium, Tin and Lead Compounds*, ed. Z. Rappoport, John Wiley & Sons, Ltd, Chichester, 2002, vol. 2, part 1, ch. 4, p. 283; (f) V. Y. Lee, K. McNeice, Y. Ito and A. Sekiguchi, *Chem. Commun.*, 2011, **47**, 3272–3274; (g) M. Zirngast, M. Flock, J. Baumgartner and C. Marschner, *J. Am. Chem. Soc.*, 2009, **131**, 15952–15962; (h) C. Jones, C. Schulten and A. Stasch, *Inorg. Chem.*, 2008, **47**, 1273–1278.
- 5 For selected reviews see: (a) K. K. Milnes, L. C. Pavelka and K. M. Baines, *Chem. Soc. Rev.*, 2016, **45**, 1019–1035; (b) N. Tokito and R. Okazaki, in *The Chemistry of Organic Germanium, Tin and Lead Compounds*, ed. Z. Rappoport, John Wiley & Sons, Ltd, Chichester, 2002, vol. 2, part 1, ch. 13, p. 843; (c) J. Escudie and H. Ranaivonjatovo, *Adv. Organomet. Chem.*, 1999, **44**, 113–174; (d) K. M. Baines and W. G. Stibbs, *Adv. Organomet. Chem.*, 1996, **39**, 275–324.
- 6 For related reactivity including germanium see: (a) V. Huch and D. Scheschewitz, *Angew. Chem., Int. Ed.*, 2013, **52**, 12179–12182; (b) W. J. Leigh, I. G. Dumbra and F. Lollmahomed, *Can. J. Chem.*, 2006, **84**, 934–948; (c) W. J. Leigh, F. Lollmahomed and C. R. Harrington, *Organometallics*, 2006, **25**, 2055–2065; (d) W. J. Leigh and C. R. Harrington, *J. Am. Chem. Soc.*, 2005, **127**, 5084–5096; (e) V. Y. Lee, M. Ichinohe and A. Sekiguchi, *J. Organomet. Chem.*, 2001, **636**, 41–48; (f) V. Y. Lee, M. Ichinohe and A. Sekiguchi, *J. Am. Chem. Soc.*, 2000, **122**, 12604–12605; (g) K. Mochida, T. Kayamori, M. Wakasa, H. Hayashi and M. P. Egorov, *Organometallics*, 2000, **19**, 3379–3386; (h) N. Fukaya, M. Ichinohe and A. Sekiguchi, *Angew. Chem., Int. Ed.*, 2000, **39**, 3881–3884; (i) S. A. Batcheller and S. Masamune, *Tetrahedron Lett.*, 1988, **29**, 3383–3384; (j) N. Fukaya, M. Ichinohe, Y. Kabe and A. Sekiguchi, *Organometallics*, 2001, **20**, 3364–3366; (k) K. L. Hurni and K. M. Baines, *Chem. Commun.*, 2011, **47**, 8382–8384.
- 7 For examples see: (a) O. M. Nefedov, M. P. Egorov, A. M. Gal'Minas, S. P. Kolesnikov, A. Krebs and J. Berndt, *J. Organomet. Chem.*, 1986, **301**, C21–C22; (b) G. Billeb, W. P. Neumann and G. Steinhoff, *Tetrahedron Lett.*, 1988, **29**, 5245–5248; (c) G. Billeb, H. Brauer, W. P. Neumann and M. Welsbeck, *Organometallics*, 1992, **11**, 2069–2074; (d) M. Kajitani, S. Adachi, C. Takayama, M. Sakurada, M. Yamazaki, T. Akiyama and A. Sugimori, *Organometallics*, 1997, **16**, 2213–2215; (e) W. Ando, H. Ohgaki and Y. Kabe, *Angew. Chem., Int. Ed. Engl.*, 1994, **33**, 659–661; (f) H. Ohgaki, N. Fukaya and W. Ando, *Organometallics*, 1997, **16**, 4956–4958; (g) W. J. Leigh, C. R. Harrington and I. Vargas-Baca, *J. Am. Chem. Soc.*, 2004, **126**, 16105–16116.
- 8 T. Ohtaki and W. Ando, *Organometallics*, 1996, **15**, 3103–3105.
- 9 K. Mochida, H. Karube, M. Nanjo and Y. Nakadaira, *J. Organomet. Chem.*, 2005, **690**, 2967–2974.
- 10 (a) M. Weidenbruch, A. Hagendorn, K. Peters and H. G. von Schnering, *Angew. Chem., Int. Ed. Engl.*, 1995, **34**, 1085–1086; (b) W. Ando and T. Tsumuraya, *J. Chem. Soc., Chem. Commun.*, 1989, 770–772.
- 11 A. Krebs, A. Jacobsen-Bauer, E. Haupt, M. Veith and V. Huch, *Angew. Chem., Int. Ed. Engl.*, 1995, **28**, 603–604.
- 12 (a) M. Veith and M. Grosser, *Z. Naturforsch., B: Anorg. Chem. Org. Chem.*, 1982, **37**, 1375; (b) M. Veith, *Angew. Chem., Int. Ed. Engl.*, 1987, **26**, 1–14; (c) M. Veith, *Angew. Chem., Int. Ed. Engl.*, 1975, **14**, 263–264.
- 13 A. Krebs and J. Berndt, *Tetrahedron Lett.*, 1983, **24**, 4083–4086.
- 14 M. P. Egorov, S. P. Kolesnikov, Yu. T. Struchkov, M. Yu. Antipin, S. V. Sereda and O. M. Nefedov, *J. Organomet. Chem.*, 1985, **290**, C27–C30.
- 15 J. Böserle, R. Jambor, A. Růžicka and L. Dostál, *RSC Adv.*, 2016, **6**, 19377–19388.
- 16 (a) K. B. Wiberg and R. E. Rosenberg, *J. Phys. Chem.*, 1992, **96**, 8282–8292; (b) N. C. Craig, S. S. Borick, T. R. Tucker and Y. Z. Xiao, *J. Phys. Chem.*, 1991, **95**, 3549–3558.
- 17 (a) C. E. Anson, N. Sheppard, R. Pearman, J. R. Moss, P. Stössel, S. Koch and J. R. Norton, *Phys. Chem. Chem. Phys.*, 2004, **6**, 1070–1076; (b) J. Krause, K. J. Haack, K. R. Pörschke, B. Gabor, C. Pluta and K. Seevogel, *J. Am. Chem. Soc.*, 1996, **118**, 804–821; (c) K. B. Borisenko, M. Broschag, I. Hargittai, T. M. Klapötke, D. Schröder, A. Schulz, H. Schwarz, I. C. Tornieporth-Oetting and P. S. White, *J. Chem. Soc., Dalton Trans.*, 1994, 2705–2712; (d) C. S. Liu, J. L. Margrave and J. C. Thompson, *Can. J. Chem.*, 1972, **50**, 465–473.
- 18 (a) M. Pavlišta, R. Bina, Z. Černošek, M. Erben, J. Vinklárík and I. Pavlík, *Appl. Organomet. Chem.*, 2005, **19**, 90–93;



- (b) E. Diana, R. Rossetti, P. L. Stanghellini and S. F. A. Kettle, *Inorg. Chem.*, 1997, **36**, 382–391.
- 19 (a) P. Pyykkö and M. Atsumi, *Chem. – Eur. J.*, 2009, **15**, 186–197; (b) P. Pyykkö and M. Atsumi, *Chem. – Eur. J.*, 2009, **15**, 12770–12779; (c) P. Pyykkö, S. Riedel and M. Patzschke, *Chem. – Eur. J.*, 2005, **11**, 3511–3520.
- 20 P. Zanello, *Inorganic Electrochemistry, Theory, Practice and Application*, RSC, Cambridge, 2003, ch. 4, pp. 159–216.
- 21 M. B. Robin and P. Day, *Adv. Inorg. Chem. Radiochem.*, 1967, **10**, 247–422.
- 22 B. Floris and P. Tagliatesta, *J. Chem. Res., Synop.*, 1993, 42–43.
- 23 M. A. Hanson, V. N. Staroverov and K. M. Baines, *Can. J. Chem.*, 2015, **93**, 134–142.
- 24 (a) T. Sugahara, J.-D. Guo, T. Sasamori, Y. Karatsu, Y. Furukawa, A. E. Ferao, S. Nagase and N. Tokitoh, *Bull. Chem. Soc. Jpn.*, 2016, **89**, 1375–1384; (b) L. Zhao, C. Jones and G. Frenking, *Chem. – Eur. J.*, 2015, **21**, 12405–12413; (c) C. Cui, M. M. Olmstead and P. P. Power, *J. Am. Chem. Soc.*, 2004, **126**, 5062–5063.
- 25 S. Yao, C. van Wullen and M. Driess, *Chem. Commun.*, 2008, 5393–5395.
- 26 (a) S. P. Green, C. Jones, P. C. Junk, K.-A. Lippert and A. Stasch, *Chem. Commun.*, 2006, 3978–3980; (b) S. Nagendran, S. S. Sen, H. W. Roesky, D. Koley, H. Grubmüller, A. Pal and R. Herbst-Irmer, *Organometallics*, 2008, **27**, 5459–5463.
- 27 B. R. Streit and D. K. Geiger, *J. Chem. Educ.*, 2005, **82**, 111–115.
- 28 (a) M. Rosenblum, N. Brawn, J. Papenmeier and M. Applebaum, *J. Organomet. Chem.*, 1966, **6**, 173–180; (b) J. Polin, H. Schottenberger, B. Anderson and S. F. Martin, *Org. Synth.*, 1996, **73**, 262–269.
- 29 G. Doisneau, G. Balavonie and T. Fillebeen-Khan, *J. Organomet. Chem.*, 1995, **425**, 113–117.
- 30 V. P. Dyadchenko, M. A. Dyadchenko, V. N. Okulov and D. A. Lemenovskii, *J. Organomet. Chem.*, 2012, **696**, 468.
- 31 M. Kotora, D. Nečas and P. Štěpnička, *Collect. Czech. Chem. Commun.*, 2003, **68**, 1897–1903.
- 32 H. Egger and K. Schlögl, *Monatsh. Chem.*, 1964, **95**, 1750–1758.
- 33 M. S. Inkpen, A. J. P. White, T. Albrecht and N. J. Long, *Chem. Commun.*, 2013, **49**, 5663–5665.
- 34 F. Barrière and W. E. Geiger, *J. Am. Chem. Soc.*, 2006, **128**, 3980–3989.
- 35 M. J. Frisch, *et al.*, *Gaussian 09, Revision B.01*, Gaussian, Inc., Wallingford CT, 2010.
- 36 Y. Zhao and D. G. Truhlar, *Theor. Chem. Acc.*, 2008, **120**, 215–241.
- 37 (a) N. Godbout, D. R. Salahub, J. Andzelm and E. Wimmer, *Can. J. Chem.*, 1992, **70**, 560–571; (b) C. Sosa, J. Andzelm, B. C. Elkin, E. Wimmer, K. D. Dobbs and D. A. Dixon, *J. Phys. Chem.*, 1992, **96**, 6630–6636.
- 38 J. Vrána, S. Ketkov, R. Jambor, A. Růžicka, A. Lyčka and L. Dostál, *Dalton Trans.*, 2016, **45**, 10343–10354.
- 39 (a) C. Peng and H. B. Schlegel, *Isr. J. Chem.*, 1993, **33**, 449–454; (b) C. Peng, P. Y. Ayala, H. B. Schlegel and M. J. Frisch, *J. Comput. Chem.*, 1996, **17**, 49–56.
- 40 J. Tomasi, B. Mennucci and R. Cammi, *Chem. Rev.*, 2005, **105**, 2999–3093.
- 41 (a) J. Ho, A. Klamt and M. L. Coote, *J. Phys. Chem. A*, 2010, **114**, 13442; (b) R. F. Ribeiro, A. V. Marenich, C. J. Cramer and D. G. Truhlar, *J. Phys. Chem. B*, 2011, **115**, 14556–14562.
- 42 (a) S. F. Boys and F. Bernardi, *Mol. Phys.*, 1970, **19**, 553–566; (b) S. Simon, M. Duran and J. J. Dannenberg, *J. Chem. Phys.*, 1996, **105**, 11024–11031.
- 43 A. E. Reed, L. A. Curtiss and F. Weinhold, *Chem. Rev.*, 1988, **88**, 899–926.
- 44 (a) R. F. W. Bader, *Atoms in Molecules: A Quantum Theory*, Oxford University Press, Oxford UK, 1990; (b) F. Cortes-Guzman and R. F. W. Bader, *Coord. Chem. Rev.*, 2005, **249**, 633–662.
- 45 T. A. Keith, *AIMAll (Version 13.05.06)*, TK Gristmill Software, Overland Park KS, USA, 2013, <http://aim.tkgristmill.com>.
- 46 (a) T. Lu and F. Chen, *J. Comput. Chem.*, 2012, **33**, 580–592; (b) T. Lu and F. Chen, *J. Mol. Graphics Modell.*, 2012, **38**, 314–323.
- 47 Z. Otwinowski and W. Minor, *Methods Enzymol.*, 1997, **276**, 307–326.
- 48 P. Coppens, in *Crystallographic Computing*, ed. F. R. Ahmed, S. R. Hall and C. P. Huber, Munksgaard, Copenhagen, 1970, p. 255.
- 49 G. M. Sheldrick, *SADABS*, Bruker AXS Inc., Madison, Wisconsin, USA, 2002.
- 50 A. Altomare, G. Casciarano, C. Giacovazzo and A. Guagliardi, *J. Appl. Crystallogr.*, 1994, **27**, 1045–1050.
- 51 G. M. Sheldrick, *Acta Crystallogr., Sect. A: Fundam. Crystallogr.*, 2015, **71**, 3–8.
- 52 G. M. Sheldrick, *SHELXL-97*, University of Göttingen, Göttingen, 2014.
- 53 A. L. Spek, *Acta Crystallogr., Sect. C: Cryst. Struct. Commun.*, 2015, **71**, 9–18.

